POLITECNICO DI MILANO
FACULTY OF ENGINEERING
DEPARTMENT OF MECHANICAL ENGINEERING

DYNAMIC ANALYSIS OF A PLANAR 2-DoF MANIPULATOR DRIVEN BY PNEUMATIC ACTUATORS

Supervisors:

1. Eng. Hermes Giberti, and
2. Ing. Simone Cinquemani

Thesis By:

Mhretie Molalign M.

Academic year 2009/2010

Abstract

In recent years, parallel manipulators have become increasingly popular in industries, especially, in the field of machine tools handling and, pick and place operations. In this thesis work, a planar 2-degree-of-freedom *(DoF)* parallel-kinematic-mechanism *(PKM)* manipulator, which is actuated by a pair of pneumatic drives is proposed. A full kinematic analysis of the manipulator is discussed in reference with a desired trajectory and motion law. In this analysis it is shown that the inverse and forward kinematics can be described in closed form; the velocity equation, singularity, and workspace of the manipulator are presented. Furthermore, the inverse dynamics analysis of the PKM manipulator is investigated employing the Newton-Euler approach, which targets on getting the desired driving force that should be applied at the joints by the actuators. After determining the drive forces, a model of pneumatic actuator is designed, which consists of models for a standard FESTO DGP/DGPL 32 linear actuator and for a 5/3 MYPE 1/8 proportional valve. The main work for analysis of the proposed planar manipulator is done in a Matlab/Simulink environment. In addition, a 3D physical model of the PKM manipulator which is created in a Solidworks graphic interface and then translated into a Simulink/Simmechanics environment has been used in both the kinematic and dynamic analysis stages. A numerical simulation of the manipulator is done based on the models created and the desired trajectory and law of motion chosen. Primary results obtained from this simulation are discussed, giving particular attention to the position error. And finally, an appropriate control strategy is designed meant to reduce the resulting error in position of the end-effector. At the end, a comprehensive conclusion of the entire work is presented and necessary recommendations are forwarded.

Acknowledgement

I am heartily thankful to my supervisors, **Eng Hermes Giberti** and **Ing Simone Cinquemani**, whose encouragement, guidance and support from the initial to the final level enabled me to develop an understanding of the subject. I would like to thank ***Politecnico di Milano*** for the facilities and support I gained from, in number of ways. I am very grateful to my family and dear friends for the encouragement and huge assistance I have been getting from you.

Lastly, I offer my regards and blessings to all of those who supported me in any respect during the completion of the work.

Molalign Mhretie

CONTENTS

List of Figures

Nomenclatures & abbreviations

L_1	–length of legs 1 and 2
L_2	–distance between sliders
L	– actuator's maximum stroke
m	–mass of each leg
m_s	–mass of each slider
m_a	–mass of moving parts in each actuator
M	–mass of payload
$P(x, y)$	– vector of position of the end-effector
$Q(q_1, q_2)$	– vector of position of the joints
ω	–angular speed
α	–angular acceleration
ς	–Lagrange multiplier
J_i	–moment of inertia of the i^{th} leg about joint point
P_s	–supply pressure
P_e	–exhaust pressure
P_{atm}	–atmospheric pressure
P_0	–initial pressure in cylinder chambers
P_1, P_2	–pressure inside chamber 1 and 2, respectively
ΔP	–change in pressure of air in chamber 1 and 2
T_s	–supply air temperature
T_e	–exhaust air temperature
T_c	–air temperature inside the chambers
A_p	–piston cross-sectional area
V_1, V_2	–volume of air inside chamber 1 and 2, respectively
V_{10}, V_{20}	–dead-volume of air inside chamber 1 and 2, respectively
u	–servo valve command signal
y	–piston displacement
q_m	–mass flow rate of air
C_P	–constant pressure specific heat of air
C_V	–constant volume specific heat of air

$K=1.4$	–heat ratio
$R=287\ [m.K^{1}]$	–*gas* constant
$B=65\quad [Nsm^{-1}]$	–viscous friction coefficient of air
$C_d=0.8$	–valve discharge coefficient
K	–total kinetic energy
U	–total potential energy
g	–gravitational acceleration
F_B	–vector of reaction forces on the legs at the joints
F_P	–vector of reaction forces on the legs at the end-effector
F_{ext}	–vector of external forces acting on the end-effector
M_{ext}	–vector of external moments acting on the end-effector
K_P	–proportional gain of controller
K_I	–integral gain of controller
K_D	–derivative gain of controller

Abbreviations

PKM	–Parallel Kinematic Mechanism
DoF	–Degree of Freedom
PRRRP	–Prismatic _Revolute _Revolute _ Revolute_ Prismatic type joint
IKA	–Inverse Kinematic Analysis
DKA	–Direct Kinematic Analysis
IDA	–Inverse Dynamic Analysis
ODE	–Ordinary Differential Equations
PID	–Proportional _ Integral _ Derivative controller

Chapter One

1. Introduction

1.1. Background and Motivation

Robotics is a relatively young field of modern technology that crosses traditional engineering boundaries. Understanding the complexity of robots and their applications requires knowledge of mechanical engineering, electrical engineering, systems and industrial engineering, computer science, economics, and mathematics. New disciplines of engineering, such as manufacturing engineering, applications engineering, and knowledge engineering have emerged to deal with the complexity of the field of robotics and factory automation. Robots can be classified as industrial robot manipulators, mobile robots, and other autonomous mechanical systems.

The term robot was first introduced into our vocabulary by the Czech playwright Karel Capek in his 1920 play Rossum's Universal Robots, the word robota being the Czech word for work.[24] Since then the term has been applied to a great variety of mechanical devices, such as teleoperators, underwater vehicles, autonomous land rovers, etc. Virtually anything that operates with some degree of autonomy, usually under computer control, has at some point been called a robot. In this text the term robot will mean a computer controlled industrial manipulator.

This Thesis work is concerned with Parallel Kinematic Mechanism *(PKM)* type industrial robot manipulator driven by pneumatic actuators, which covers the kinematics and dynamics analysis of the *PKM* , motion planning and control of the manipulator under different desired trajectories.

A parallel manipulator consists of a moving platform and a fixed base, connected by several linkages (also called legs). As PKM are used for more difficult tasks, control requirements increase in complexity to meet these demands. The implementation for PKMs often differs from their serial counterparts, and the dual relationship between serial and parallel manipulators often means one technique which is simple to implement on serial manipulators is difficult for PKMs (and vice versa). Because parallel manipulators result in a loss of full constraint at singular configurations, any control applied to a parallel manipulator must avoid such configurations. The manipulator is usually limited to a subset of the usable workspace since the required actuator torques will approach infinity as the manipulator approaches a singular configuration. Thus, some method must be in place to ensure that the manipulators avoid those configurations.

Parallel robots have many advantages comparing to the serial robots, such as high flexibility, high stiffness, and high accuracy. To achieve a higher accuracy the static and dynamic behavior must be better understood. The problems concerning kinematics and dynamics of parallel robots are as a rule more complicated than those of serial one.

Chapter Two

2. Literature Review

2.1. Parallel manipulator Design

The conceptual design of PKM manipulators can be dated back to the time when Gough established the basic principles of a manipulator with a closed-loop kinematic structure (Gough, 1956), that can generate specified position and orientation of a moving platform so as to test tire wear and tear. Stewart designed a platform manipulator for use as an aircraft simulator in 1965 (Stewart, 1965). In 1978, Hunt (1978) made a systematic study of manipulators with parallel kinematics, in which the planar 3-RPS parallel manipulator is a typical one. Since then, parallel manipulators have been studied extensively by numerous researchers.[1]

The most studied parallel manipulators are those with 6 Degree of Freedoms (DoFs). These parallel manipulators possess the advantages of ***high stiffness, low inertia, and large payload capacity***. However, they suffer the problems of relatively ***small useful workspace*** and ***design difficulties*** (Merlet, 2000). Furthermore, their direct kinematics pose a very difficult problem; however the same problem of parallel manipulators with 2 and 3 DoFs can be described in ***closed form*** (Liu, 2001. Moreover, for a parallel manipulator with 2 and 3 DoFs, the ***singularities*** can always be identified readily. For such reasons, parallel manipulators with, especially 2 and 3 DoFs, have increasingly attracted more and more researchers' attention with respect to industrial applications (Tonshoff et al., 1999; Siciliano, 1999; Tsai and Stamper, 1996; Ceccarelli, 1997; Liu et al., 2001). In these designs, parallel manipulators with three translational DoFs have been playing important roles in the industrial applications (Tsai and Stamper, 1996; Clavel, 1988; Hervé, 1992; Kim and Tsai, 2002; Zhao and Huang, 2000; Carricato and Parenti-Castelli, 2001; Kong and Gosselin, 2002), especially, the DELTA robot (Clavel, 1988), which is evident from the fact that the design of the DELTA robot is covered by a family of 36 patents (Bonev, 2001). Tsai's manipulator (Tsai and Stamper, 1996), in which each of the three legs consists of a parallelogram, is the first design to solve the problem of UU chain. A 3-translational-DoF parallel manipulator, *Star*, was designed by Hervé based on group theory (Hervé, 1992). Such parallel manipulators have wide applications in the industrial world, e.g., pick-and-place application, parallel kinematics machines, and medical devices.

The existing planar 2-DoF parallel manipulators (Asada and Kanade, 1983; McCloy, 1990; Gao et al., 1998) are the well-known five-bar mechanism with prismatic actuators or revolute actuators. In the case of the manipulator with revolute actuators, the mechanism consists of five revolute pairs and the two joints fixed to the base are actuated. In the case of the manipulator with prismatic actuators, the mechanism consists of three revolute pairs and two prismatic joints and the prismatic joints are actuated. The output of the manipulator is the translational motion of a point on the end-effector, i.e., the orientation of the end-effector is also changed correspondingly.

2.2. Robots mechanisms and their classification

A robot is a machine capable of physical motion for interacting with the environment. Physical interactions include ***manipulation***, ***locomotion***, and any other tasks changing the state of the environment or the state of the robot relative to the environment. A robot has some form of mechanisms for performing a class of tasks. A rich variety of robot mechanisms has been developed in the last few decades.

2.2.1. Joint Primitives and Serial Linkages

A robot mechanism is a multi-body system with the multiple bodies connected together. We begin by treating each body as rigid, ignoring elasticity and any deformations caused by large load conditions. Each rigid body involved in a robot mechanism is called a ***link***, and a combination of links is referred to as a ***linkage***. In describing a linkage it is fundamental to represent how a pair of links is connected to each other. There are two types of primitive connections between a pair of links, as shown in ***Figure 2.1***, below. The first is a ***Prismatic joint*** where the pair of links makes a translational displacement along a fixed axis. In other words, one link slides on the other along a straight line. Therefore, it is also called a sliding joint. The second type of primitive joint is a ***Revolute joint*** where a pair of links rotates about a fixed axis. This type of joint is often referred to as a hinge, articulated, or rotational joint.

a) Prismatic joint b) Revolute joint

Figure 2.1 Types of primitive connections.

Combining these two types of primitive joints, one can create many useful mechanisms for robot manipulation and locomotion. These two types of primitive joints are simple to build and are well grounded in engineering design. Most of the robots that have been built so far are combinations of only these two types.

2.2.2. Robot Components

A particular kind of robot, whether Humanoid or industrial manipulator, consists of the following fundamental components.

- **Body** : the main part of the robot that helps the transformation of motion, torque or forces. In most cases, it refers to the linkages and their mechanisms
- **Effectors**: This are the last components to receive motion and enables a robot perform the desired task by interacting with the external environments. The effectors maybe of various types, the four most common ones are:
  1. ***Impactive***: – jaws or claws which physically grasp by direct impact upon the object.
  2. ***Ingressive***: – pins, needles or hackles which physically penetrate the surface of the object (used in textile, carbon and glass fiber handling).
  3. ***Astrictive:*** – suction forces applied to the objects surface (whether by vacuum, magneto– or electro adhesion).
  4. ***Contigutive***: – requiring direct contact for adhesion to take place (such as glue, surface tension or freezing).
- **Actuators**: An actuator or drive is a source of motion for a robot to perform its task. It can be of linear type(Cylinders) or rotary type(e.g. Motors). Commonly they are classified based on the kind of medium used for energy transmission., such as Electrical, Hydraulic, Pneumatic and Internal Combustion (*IC*) hybrids.
- **Sensors**: sensors are those components that helps to acquire a feedback action by interaction with the surrounding of the robot.
- **Controller**: The controllers are used to maintain the robot precision, stability, linearity and manageability within a desired appropriate limits.

2.2.3. Robotic Systems

A robot manipulator should be viewed as more than just a series of mechanical linkages. The mechanical arm is just one component in an overall Robotic System, illustrated in ***Figure 2.2***, which consists of the arm, external power source, end-of-arm tooling, external and internal sensors, computer interface, and control computer. Even the programmed software should be considered as an integral part of the overall system, since the manner in which the robot is programmed and controlled can have a major impact on its performance and subsequent range of applications.

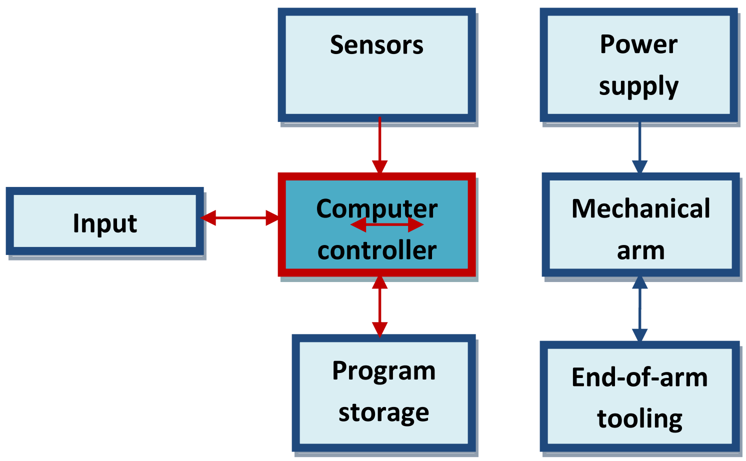

Figure 2.2 A typical robot/ manipulator functional system

2.3. Parallel Manipulator

A parallel manipulator is one in which some subset of the links form a ***closed chain***. More specifically, a parallel manipulator has two or more independent kinematic chains connecting the base to the end-effector. The closed chain kinematics of parallel robots can result in *greater structural rigidity*, and hence *greater accuracy*, than open chain robots. The kinematic description of parallel robots is fundamentally different from that of serial link robots and therefore requires different methods of analysis. [22]

A parallel mechanism is one of the most active areas of current mechatronics and robotics research. Since it is promising to have those supplementary features that serial mechanisms is in lack of such as *high rigidity*, *high stiffness*, *high accuracy*, *high speed*, *high acceleration* and *high payload*. However they are much more complicated than the serial mechanisms due the presence of closed loop constraints. And our understanding of them is far behind that of serial mechanisms, which have been extensively studied. [23]

2.4. Pneumatic drives

What is an actuator? An actuator is a mechanical device used for moving or controlling something (in this case manipulators). Generally, based the medium used to transfer energy, actuators/drive are classified as:

- Electric Motors and Drives
- Hydraulic Drives
- Pneumatic Drives
- Internal Combustion hybrids

2.4.1. Pneumatic Actuators

Most of the earlier pneumatic control systems were used in the process control industries, where the low pressure air of the order 7-bar was easily obtainable and give sufficiently fast response. Pneumatic systems are extensively used in the automation of production machinery and in the field of automatic controllers. For instance, pneumatic circuits that convert the energy of compressed air into mechanical energy enjoy wide usage, and various types of pneumatic controllers are found in industry. Certain performance characteristics such as fuel consumption, dynamic response and output stiffness can be compared for general types of pneumatic actuators, such as piston-cylinder and rotary types. Figure below shows the two types of pneumatic actuators [30] The pneumatic actuator has most often been of the piston cylinder type because of its low cost and simplicity . The pneumatic power is converted to straight line reciprocating and rotary motions by pneumatic cylinders and pneumatic motors. The pneumatic position servo systems are used in numerous applications because of their ability to position loads with high dynamic response and to augment the force required moving the loads. Pneumatic systems are also very reliable. [30]

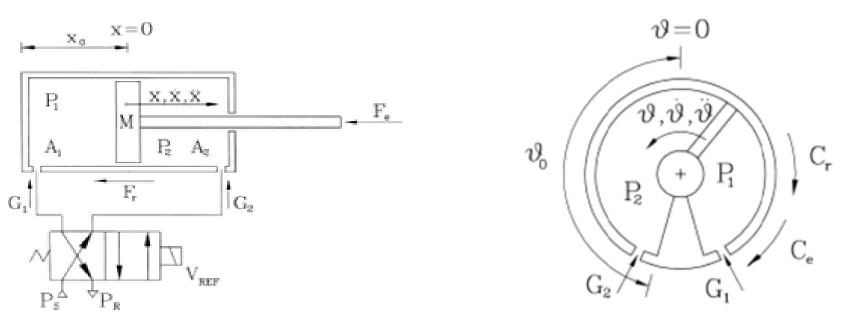

a) Double acting linear pneumatic actuator. b) Vane rotary pneumatic actuator.

Figure 2.3 The two fundamental types of pneumatic actuators

2.4.2. Pneumatic Systems

- Pneumatic systems are designed to move loads by controlling pressurized air in distribution lines and pistons with mechanical or electronic valves.
- Air under pressure possesses energy which can be released to do useful work.
- Some examples of pneumatic systems are: dentist's drill, pneumatic road drill, automated production systems.

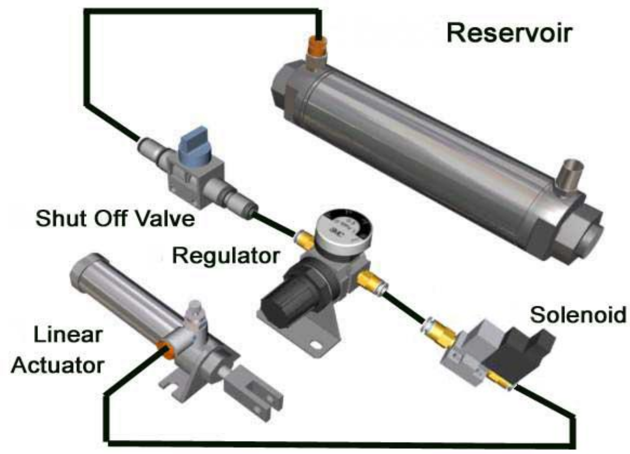

Figure 2.4 Pneumatic power supply system

2.4.3. Pneumatic Drives Characteristics

- Many of the same principles as hydraulics except working fluid is compressed air
- Compressed air widely available and environmentally friendly,
- Piping installation and maintenance is easy
- Explosion proof construction
- Major disadvantage is compressibility of air, leading to low power densities and poor control properties (usually on/off)
- Pneumatic systems are suitable for light and medium loads (30N-20kN) with temperature -40 to 200 degrees Celsius

In general pneumatic systems have the following key merits

- Low cost and easy to install
- Clean and easy to maintain
- Low power densities
- Only on/off or inaccurate control necessary

2.4.4. Pneumatic Valves

Pneumatic valve is a component placed in between the reservoir and the cylinder for the purpose of regulation the flow of air. It regulates the air flow to and from the cylinder according to an appropriate command given to it as an electrical signal. The two most common types electromechanical servo valves are the three port –two way (3-2) and the five port- three way (5-3) valves. ***Figure 2.5*** shows the very simple type of a 5-3 servo valve connected to a double action, single rod cylinder.

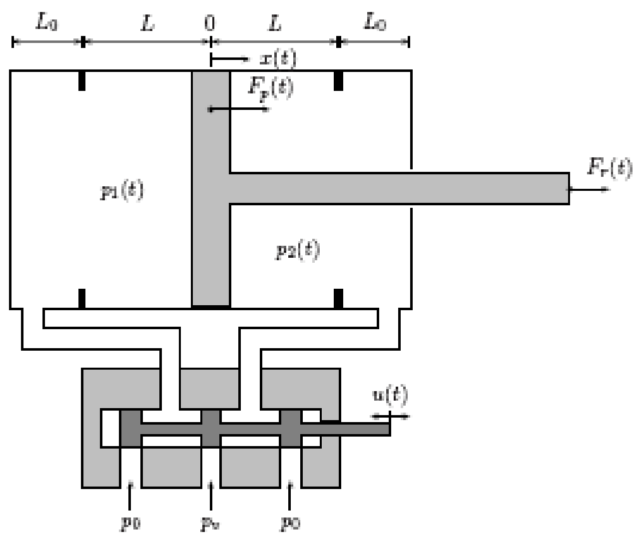

Figure 2.5 A 5-port-3-way servo valve

2.5. Solid work modeling

SolidWorks is a Parasolid-based solid modeler, and utilizes a parametric feature-based approach to create models and assemblies. It is capable of carrying out numerous tasks ranging from simple components physical modeling up to simulation, motion study and sustainability analysis of a more complex assembly. However, in this thesis work the use of Solid work is limited, it will be implemented for creating a 3D physical model of the manipulator, which principally can be translated into Matlab/Simulink-SimMechanics interface. The general step used in the modeling will be discussed in the subsequent chapter that deals with the kinematic design of the PKM manipulator.

Chapter Three

3. Kinematic Analysis

This chapter discusses the formulation of equations, assumption of constraint and boundary conditions, simplified Solidworks modeling of the PKM manipulator and how these characteristic parameters can be combined in a Matlab/Simulink environment in order to perform a kinematic analysis of the manipulator. Finally, there will be a conclusion on the results obtained from the kinematic analysis, which in fact will deal with the position traction of a desired trajectory.

3.1. Kinematic mechanism description

The PRRRP 2-DoF parallel mechanism usually consists of two legs, each of which is the PRR (R-revolute joint and P-prismatic joint) chain. The two legs are connected to the end-effector point with a common R joint. The mechanism can position at a point in a plane when the P joint in each of the two legs is actuated by a linear actuator. A PRRRP mechanism that is actuated along the Y-axis direction is shown in ***Figure 3.1.***

As illustrated in ***Figure. 3.1.*** a reference frame ***R : O- xy*** is fixed to the base. Vectors $\boldsymbol{q_i}$ *(i=1,2)* are defined as the position vectors of points $\boldsymbol{B_i}$ in frame ***R***. The geometric parameters of the mechanism are $\boldsymbol{PB_i = L_2}$ *(i = 1, 2)*, and the distance between two actuators is $\boldsymbol{2L_1}$. The position of point ***P*** in the fixed frame ***R*** is given by:

$$P = [x\ y]^T \tag{3.1}$$

As shown in ***Figure 3.1***. the position vector of the points $\boldsymbol{q_i}$ in the fixed frame ***R*** is denoted by:

$$Q = [q_1\ q_2\ ]^T \tag{3.2}$$

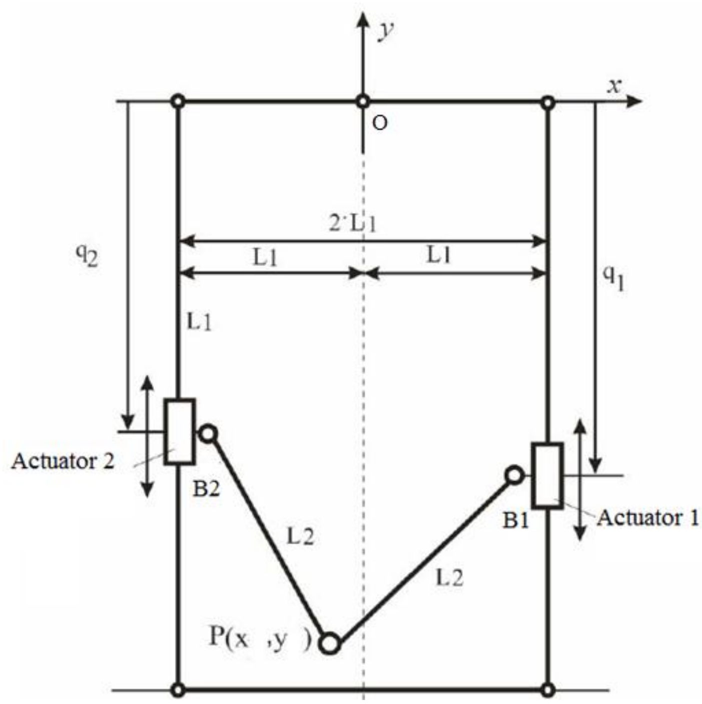

Figure 3.1 Kinematic description of the PKM manipulator

3.2. Workspace of PKM Manipulator

For determination of different characteristics of the workspace, in order to compare different existing manipulators or design a new manipulator, it is almost always necessary to determine the boundaries of the workspaces. Since workspace determination is generally an intermediate but critical step in analyzing and synthesizing manipulators, it is very important to have a theory to safeguard the estimation and conceptual design. The workspace of a manipulator is the domain of reach of its end-effector and is bounded in the 3D/2D space, depending on the DoF of the manipulator. The workspace of a manipulator has been defined in literature as the totality of positions that a particular identified point of the manipulator (end-effector) can reach. The workspace boundary is the curve (in plane) or the surface (in space) that defines the extent of reach of the end-effector.

The size of workspace has a huge impact on the possible functionality of a manipulator and it gives an insight of the performance a machine. Therefore, many scholars have proposed algebraic method and geometric method to determine the workspace of a manipulator. Wang et al. [8] presented an algorithm, called the boundary search method, to determine the workspace of a parallel machine tool. They also analyzed the boundary workspace in order to expand its operating scope.

The focuses of the many literature are mainly on finding the workspace of a manipulator, but seldom discuss the relationship between the shapes of the workspace and the geometry structure of the manipulator. There exists no theorem for spatial parallel manipulators which characterizes the geometry relationship between the reachable workspace of closed-loop manipulators and the structures of their kinematic chains. For a 2-DoF planar PKM manipulator, the workspace can be explicitly represented as a region along the horizontal (X-axis) which can be reached by the end effector without cause kinematic constraint and boundary condition violations. Hence, as shown in ***Figure 3.2.*** the workspace is a function of the arm length $\boldsymbol{L_2}$ and the distance between the two actuators $\boldsymbol{2L_1}$, for a given length of the actuator.

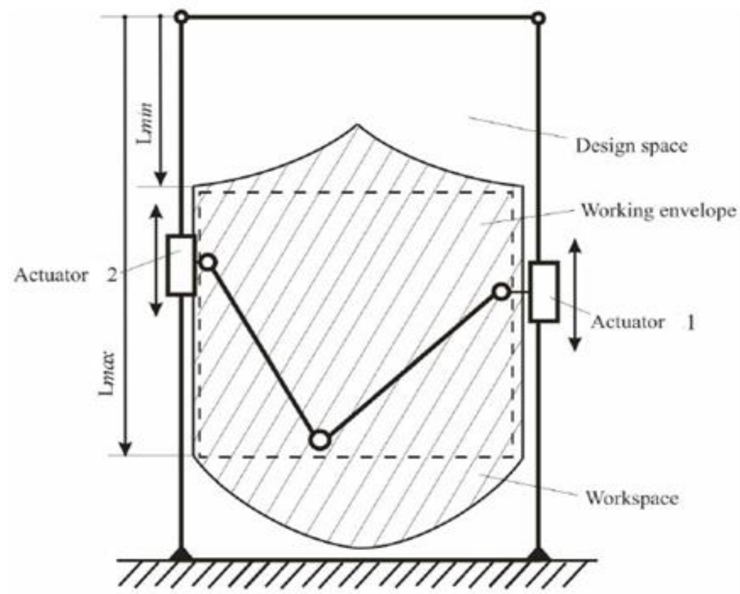

Figure 3.2 Workspace envelop for a 2 DoF planar PKM manipulator

Hence, the boundary that limits the workspace across the horizontal direction can be determined as:

$$W = 2(L_2 - L_1) \tag{3.3}$$

3.3. Inverse Kinematic Problem

The Inverse kinematic problem involves in the determination of the joint/s motion (position, velocity and acceleration) for a known value of end effector motion. Assuming that the user can generate the desired end effector motion from any trajectory of interest and an appropriate motion law, we will discuss the equation which governs the determination of joint space motion at points B_1 and B_2.

3.3.1. Position Analysis

The equations which govern the kinematic problem of the PKM are given as:

$$(x-L_1)^2+(y-q_1)^2=L_2^2 \tag{3.4}$$

$$(x+L_1)^2+(y-q_2)^2=L_2^2 \tag{3.5}$$

The inverse kinematic problem can then be written as

$$q_1=\pm\sqrt{L_2^2-(x-L_1)^2}+y \tag{3.6}$$

$$q_2=\pm\sqrt{L_2^2-(x+L_1)^2}+y \tag{3.7}$$

3.3.2. The Jacobian Matrix

Eqs. (3.4) and ***(3.5)*** can be differentiated with respect to time to obtain the velocity equations. This leads to an equation of the form:

$$\boldsymbol{A}\begin{pmatrix}\dot{q}_1\\ \dot{q}_2\end{pmatrix}=\boldsymbol{B}\begin{pmatrix}\dot{x}\\ \dot{y}\end{pmatrix} \tag{3.8}$$

where ***A*** and ***B*** are *2x2* matrices that can be expressed as

$$A=\begin{bmatrix}y-q_1 & 0\\ 0 & y-q_2\end{bmatrix}, and \qquad B=\begin{bmatrix}x-L_1 & y-q_1\\ x+L_1 & y-q_2\end{bmatrix} \tag{3.9}$$

Matrix algebra indicates that there exists a Jacobian Matrix if and only if the matrix **A** is not singular. consequently, the Jacobian matrix is obtained by

$$J=A^{-1}B=\begin{bmatrix}\frac{x+L_1}{y-q_1} & 1\\ \frac{x-L_1}{y-q_2} & 1\end{bmatrix} \tag{3.10}$$

Eqs. (3.6) and ***(3.7)*** indicates that there are two different possible motions for each joint. For the working mode as shown in ***Figure. 3.1*** that the ''±'' in ***Eqs. (3.6)*** and ***(3.7)*** are both ''+'', and the Jacobian matrix can be rewritten as:

$$J=\begin{bmatrix}\frac{x+L_1}{\sqrt{L_2^2-(x+L_1)^2}} & 1\\ \frac{x-L_1}{\sqrt{L_2^2-(x-L_1)^2}} & 1\end{bmatrix} \tag{3.11}$$

3.3.3. Velocity and Acceleration Analysis

Having the position vectors of the end-effector ***P*** and the joints ***Q*** from ***Eq. (3.1)*** and ***Eq. (3.2)***, respectively, and then, with direct kinematic analysis the end effector position ***P*** can be stated as a function of the joint position ***Q*** by a set of closed-form equations.

$$P = F(Q) \tag{3.12}$$

Consequently, the joint space velocities at the slider-leg junctions, point B_1 and B_2 can be calculated as follows

$$\dot{Q} = J\dot{P} \tag{3.13}$$

Where ***J*** is the Jacobian matrix obtained in ***Eq. (3.11)***. Similarly the joint space acceleration can be obtained from the known end-effector motion and the already determined joint position ***Q*** and joint velocity $\dot{\boldsymbol{Q}}$.

$$\ddot{Q} = J\ddot{P} + \hat{A}(Q, \dot{Q}) \tag{3.14}$$

where

$$\hat{A} = \begin{bmatrix} \frac{\dot{x}^2+\dot{y}^2-2\dot{y}\dot{q}_1+\dot{q_1}^2}{y-q_1} \\ \frac{\dot{x}^2+\dot{y}^2-2\dot{y}\dot{q}_2+\dot{q_2}^2}{y-q_2} \end{bmatrix} \tag{3.15}$$

3.4. Direct Kinematic Problem

3.4.1. Direct analysis for position

The direct kinematic analysis is concerned about obtaining the end-effector motion (Position, velocity and acceleration) when the joint motion is given or known from the output of actuators. In this case, for the position of the end-effector the value of ***x*** and ***y*** can be found as follows as a function of the joint positions q_1 and q_2.

$$y = -\frac{d-\sqrt{(d^2-4c\cdot d)}}{2c} \tag{3.16}$$

$$a = \frac{(q_2 - q_1)}{2R_1}; \qquad b = \frac{(q_1^2 - q_2^2)}{4L_1}; \qquad c = a^2 + 1; \qquad d = (b - L_1)^2 + q_1^2 - R_2^2;$$

$$e = 2a(b - L_1) - 2q_1$$

$x = L_1 + \sqrt{L_2^2 - (y - q_1)^2}$
(3.17)

3.4.2. Direct analysis for velocity and acceleration

The end-effector velocity and acceleration can be determined from the joints motion. And, the equations which govern this analysis are given below in ***Eq. (3.18)*** and ***(3.19),*** respectively.

$$\dot{P} = J^{-1}\dot{Q} \quad (3.18)$$

$$\ddot{P} = J^{-1}[\ddot{Q} - \hat{A}(Q, \dot{Q})] \quad (3.19)$$

3.5. Singularity Conditions

Most of the times, kinematic singularity leads to a loss of the controllability and degradation of the natural stiffness of manipulators, as a result the analysis of parallel manipulators has drawn considerable attention. In some configurations, the robot cannot be fully controlled. Most parallel manipulator suffer from the presence of singular configurations in their workspace that limit the machine performances. In the case of parallel manipulators and closed-loop mechanisms, singularity analysis is much more difficult since such mechanisms contain unactuated joints and joints with more than one degree of freedom[ref4]. In general, closed-form solutions for singular curves/surfaces for parallel manipulators of arbitrary architecture requires elimination of unwanted variables from several nonlinear transcendental equations, and this is quite difficult.

Based on the forward and inverse Jacobian matrices, three kinds of singularities of parallel manipulators can be obtained [24]. Let ***q*** denote the actuated joint variables, and let ***p*** describe the location of the moving platform. The kinematic constraints imposed by the arms of the manipulator are expressed as ***f(x, q)=0***. Differentiating with respect to time, a relation between the input joint rates and the end effector output velocity is obtained as:

$$J_p\dot{p} = J_q\dot{q} \quad (3.20)$$

Where, $J_p = \frac{\partial f}{\partial p}$ and $J_q = \frac{\partial f}{\partial q}$. Which leads to the overall Jacobian matrix J, can be written as:

$$J = {J_q}^{-1}J_p \quad (3.21)$$

It is said that singular configurations should be avoided at any cost. The singular configurations (also called singularities) of a parallel robot may appear inside the workspace or at its boundaries.

3.5.1. The first kind of singularity

The first kind of singularity occurs when the following condition is satisfied:

$$\det(J_p) = 0\,, \qquad \det(J_q) \neq 0$$

This kind of singularity corresponds to the limit of the workspace. Where, the end-effector point P moves to either extremes sides of the work envelop resulting in constraint violation.

3.5.2. The second kind of singularity

The second kind of singularity occurs when we have following:

$$\det(J_p) = 0\,, \quad \det(J_q) \neq 0$$

The physical interpretation of this kind of singularity is that even if all of the input velocities are zero, there are still be instantaneous motion of the end-effector. In this configuration, the manipulator loses stiffness and becomes uncontrollable. This kind of singularity is located inside the workspace of the manipulator. Such a singularity is very difficult to locate only by analyzing and expanding the equation $\det(J_q) = 0$. A numerical method is thus a good selection for solving this problem.

3.5.3. The third kind of singularity

The third kind of singularity occurs when both:

$$\det(J_p) = \det(J_q) = 0$$

This kind of singularity corresponds to the first and second type of singularity occurring simultaneously. This singularity is both configuration and architecture dependent.

Parallel singularities are particularly undesirable because they cause the following problems:

- a high increase of forces in joints and links, that may damage the structure,
- a decrease of the mechanism stiffness that can lead to uncontrolled motions of the tool though actuated joints are locked. [44]

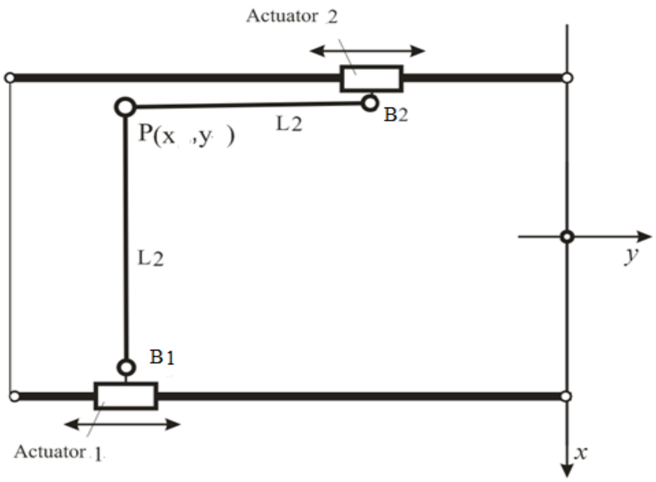

Figure 3.3 Singularity configuration of a PKM 2-DoF manipulator

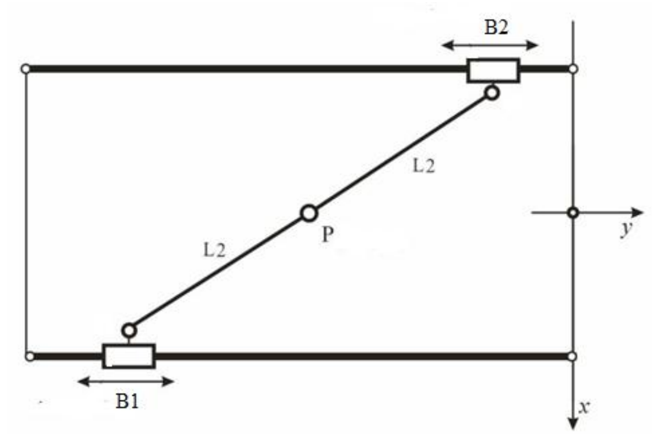

Figure 3.4 Singularity configuration of a PKM 2-DoF manipulator

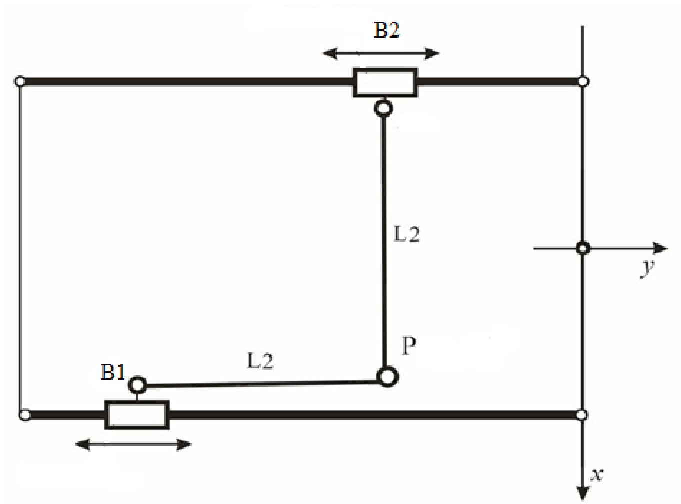

Figure 3.5 Singularity configuration of a PKM 2-DoF manipulator

3.6. Solidworks modeling

Before leading to the full inverse kinematic analysis in Matlab/Simulink it is necessary to create a physical model of the manipulator in Solidworks environment, and then, to translate that into a Matlab/Simulink-SimMechanics compatible format. All the dimensions of the robot are assumed to be as follows:

$2*L_1$ = ***500 mm*** is the distance between sliders

L = ***1500 mm*** is the length of both the cylinders (maximum stroke)

L_2 = ***354 mm*** is the length of the two arms

d=***30 mm*** is the diameter of the arm rods

d_c=***32 mm*** is the bore diameter of the cylinder

The three dimensional (3D) model built in Solidworks in shown below in ***Figure 3.6***. Each of the components are created separately in Solidworks components design module as shown in ***Figure 3.7***, and then brought together in the assembly module to create the complete manipulator. Though it is possible to study the kinematics of the manipulator in Solidworks environment, it has not tried here because it is more direct and understandable in a Matlab/Simulink environment.

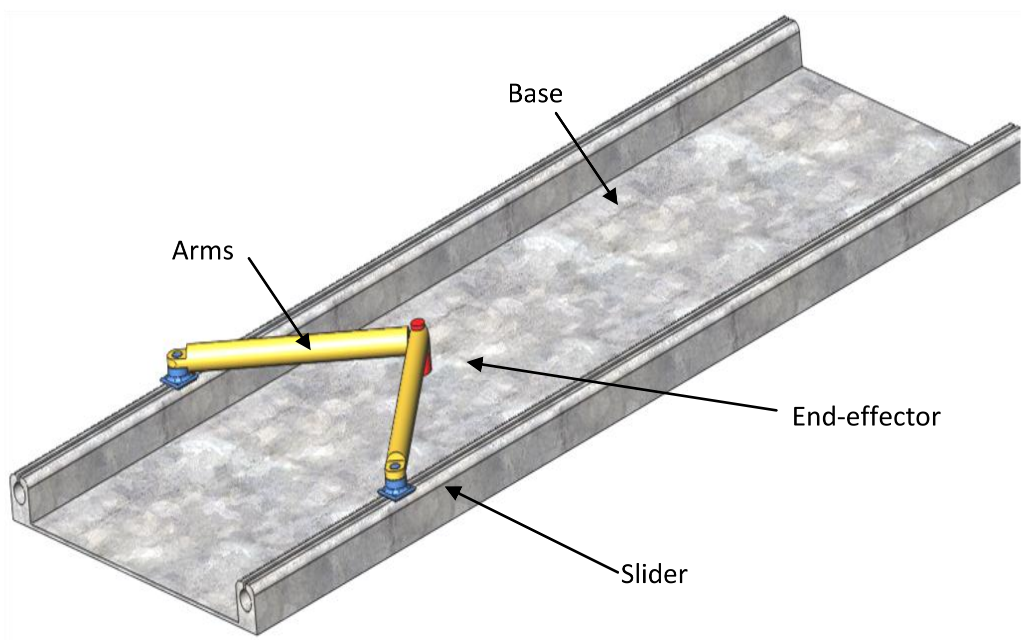

Figure 3.6 A 3D physical model of the complete PKM manipulator created with Solidworks

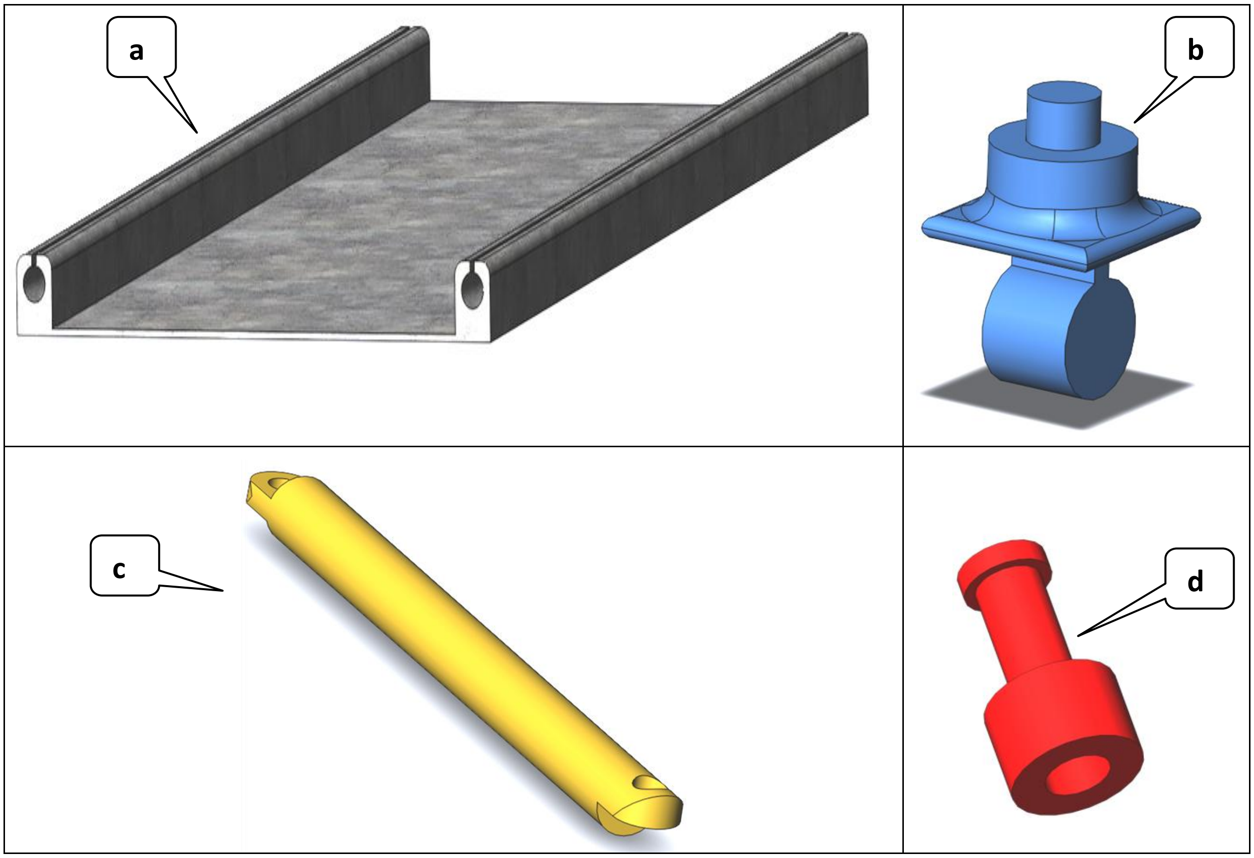

Figure 3.7 Solidworks individual component model for the PKM manipulator

a) Base
b) Slider
c) Arm and
d) End-effector

3.7. Numerical Simulation for the Inverse Kinematic Analysis

For the Kinematic analysis, a model is developed in Simulink including the physical model of the manipulator designed in Solidworks (shown in ***Figure 3.6***) and exported to Simulink-SimMechanics. The necessary steps and assumptions for the development of a physical model in Solidworks are discussed in the previous chapter under the topic Solidworks modeling, hence here it is only presented the final entire model of the manipulator. ***Figure 3.8,*** below, shows the complete Matlab/Simulink + Solidworks model developed for the kinematic analysis of the parallel manipulator

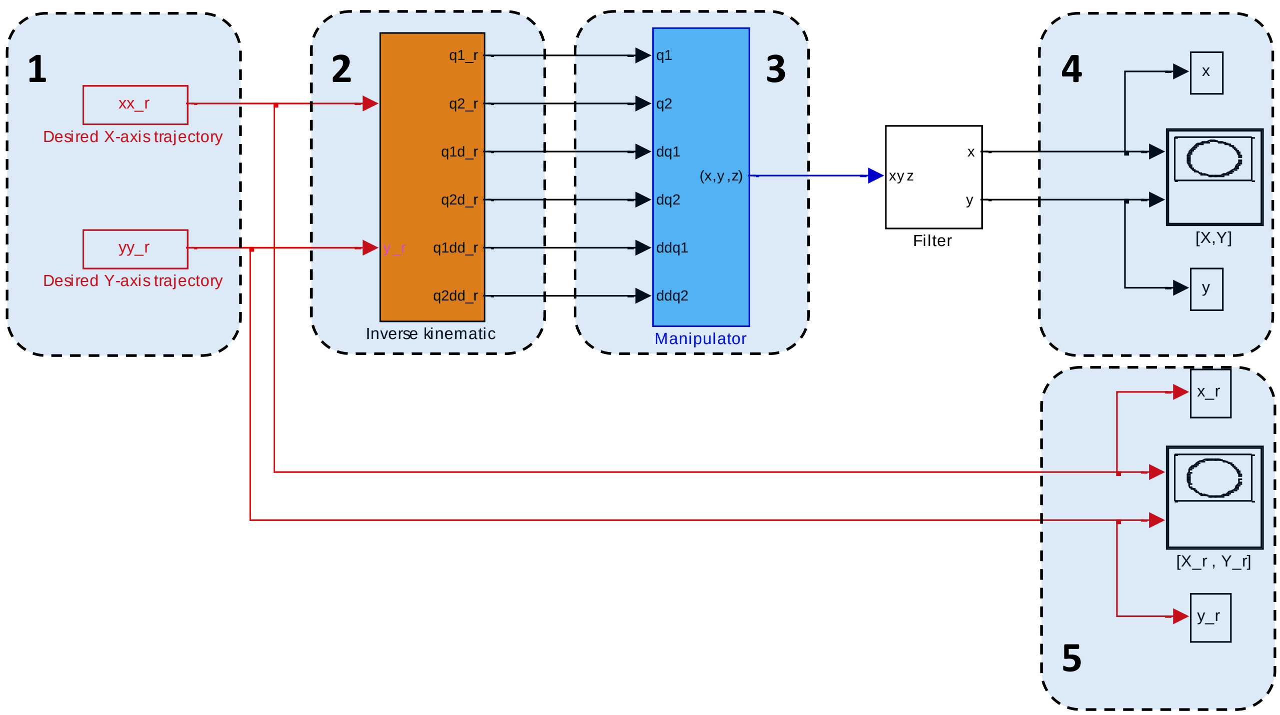

Figure 3.8 A complete model of the PKM manipulator on a Simulink environment

3.7.1. Description of sections in Simulink model

Section 1: This section has contained the input to the program. It is the vector of the desired trajectory ***X-axis*** and ***Y-axis*** components against the motion time ***t***. In general these inputs are functions of all known parameters, such as: the desired trajectory, the desired motion law and the motion time. More on the choice of motion law will be discussed in chapter 5 .However, at this stage a circle of radius $r=100mm$ is used as the desired trajectory. Whereas, the law of motion is assumed to be a symmetric constant acceleration law with a motion time of $T=10$ seconds.

Section 2: This section is the major step in the Inverse Kinematic Analysis (*IKA*) of the manipulator. Through the inverse Kinematic Analysis equations discussed above, the joint space motion is determined as a function of the end-effector [P(x, y)] motion. The mathematical algorism which cover this section in written in the ***Matlab*** code file which is namedas *main_kinematic.m.* For more detail regarding the implemented Matlab codes the reader is advised to refer to the functions given in ***Appendix-A Part I***. Similarly, the IKA can totally be done in ***Simulink*** space as shown in ***Figure 3.9***, blow.

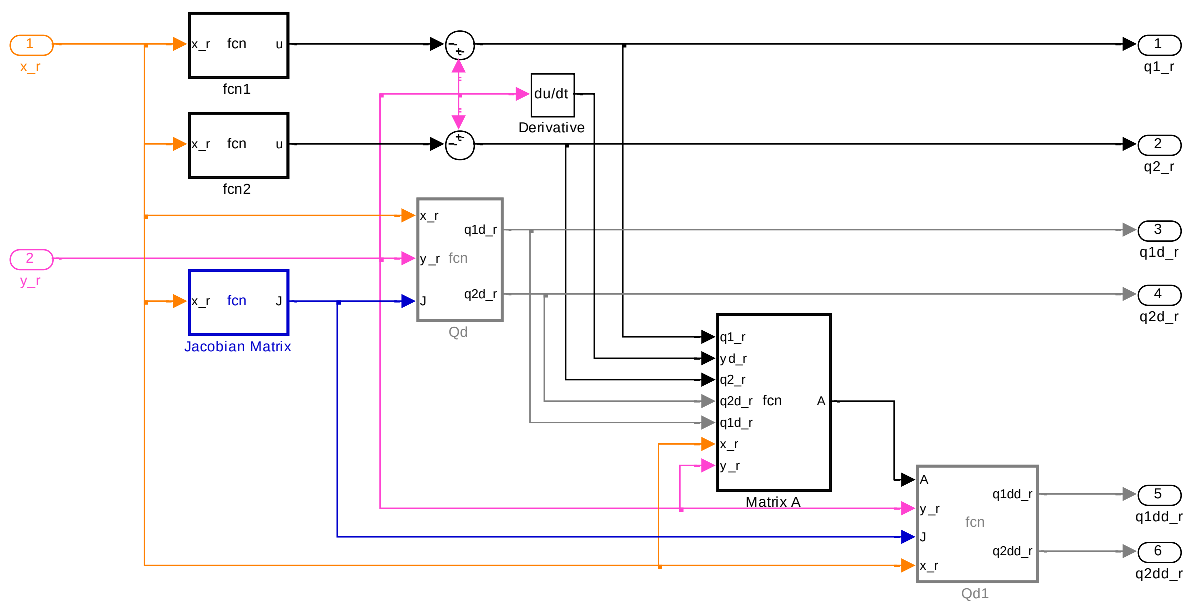

Figure 3.9 Inverse Kinematic Analysis (IKA):- Simulink based model

Section 3: In this section, the physical model created in Solidworks and transformed in to Matlab/Simulink environment is provided with the necessary motion input at the joints. It introduces functions $f_1(q_1, \dot{q}_1, \ddot{q}_1)$ and $f_2(q_2, \dot{q}_2, \ddot{q}_2)$ at points B_1 and B_2 , respectively, and induces a kinematic simulation of the PKM manipulator. ***Figure 3.10***, below, shows the translated model in a Simulink-SimMechanics environment.

Section 4: This section display the resulting trajectory simulation while the main program is executed. It is designed to display all the trajectory points in an X-Y plane plot, which in deed is lied inside the workspace of the PKM manipulator.

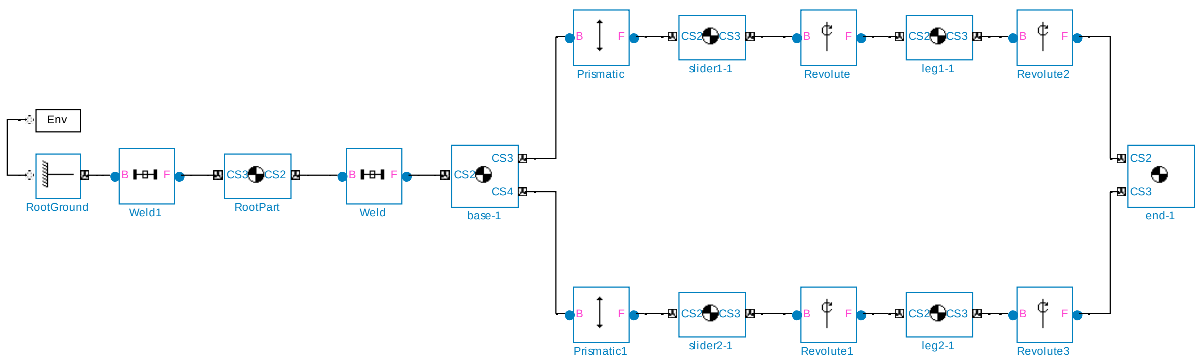

Figure 3.10 Model of PKM Manipulator in a SimMechanics interface

The same model with all the input motions applied at joints 1 and 2, is shown in ***Figure 3.11***. In this model, the mechanical system is given a genaralized motion (position, velocity and aceeleration) at the joints through a SimMechanics library block *joint actuator* attached to prisimatic joints and the response motion is obtained through *body sensors* block attached to any of the desired linkages.

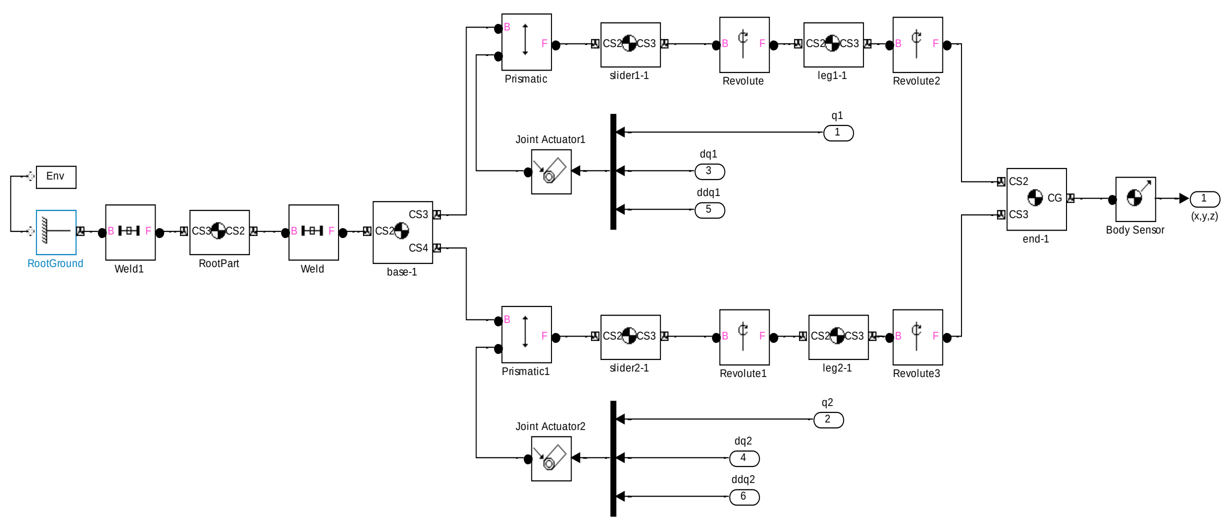

Figure 3.11 Model in Simmechanics with desired motion as an input for kinematic analysis

Section 5: This section gives the simulated plot of the desired trajectory given by the user as an input, by a similar fashion discussed in *section 4*, above.

3.7.2. Results and discussions

Both the Matlab based and Simulink based analysis results in same output. The desired trajectory, assumed to be a circle, is shown in ***Figure 3.12*** below,

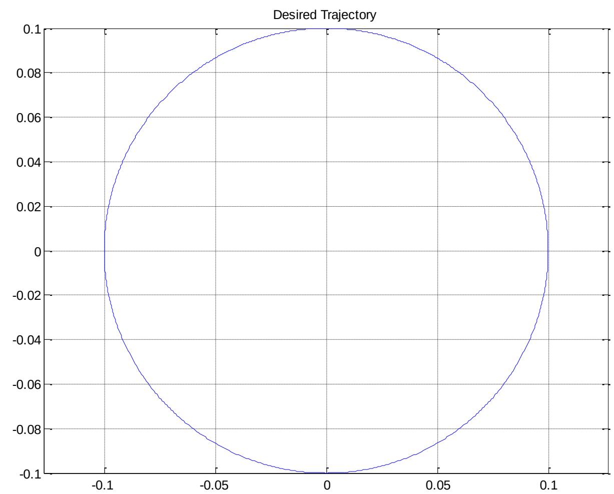

Figure 3.12 Desired Trajectory

Whereas, the plot of a symmetric constant acceleration law, which is chosen to be the governing motion law for the kinematic analysis is given in ***Figure 3.13***.

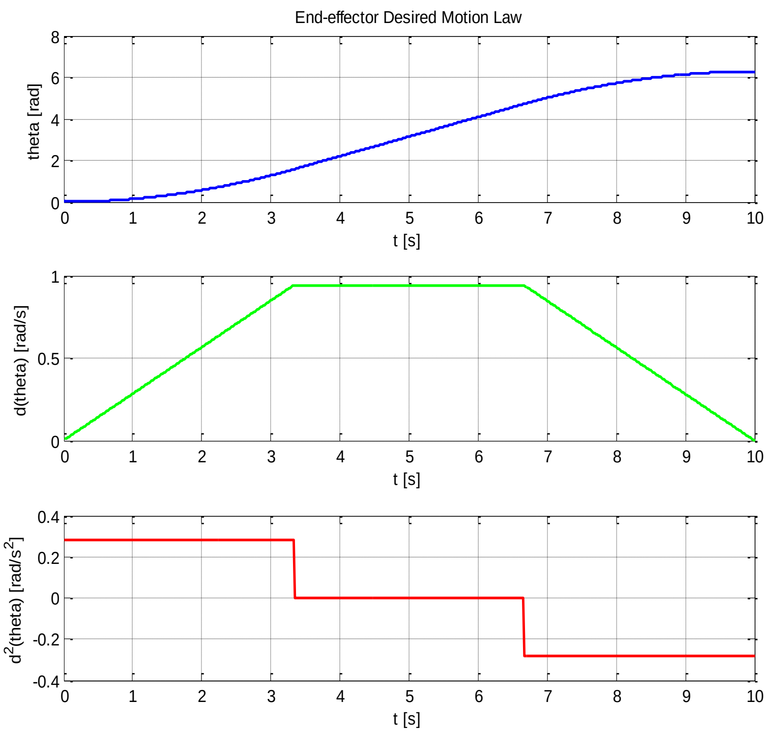

Figure 3.13 Desired motion law (A symmetric Constant Acceleration Law)

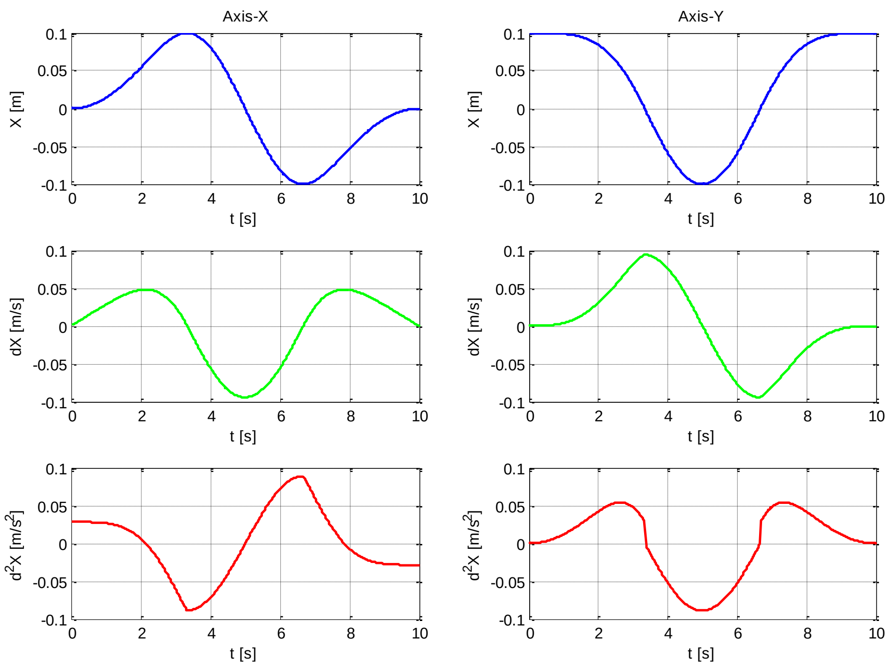

Figure 3.14 Desired motion law of the end effector

Figure 3.14, above depicted the desired motion of the end-effector, actually decomposed into its components along the x-axis and y-axis; and ***Figure 3.15*** below, shows the profile of the desired motion in the joint space.

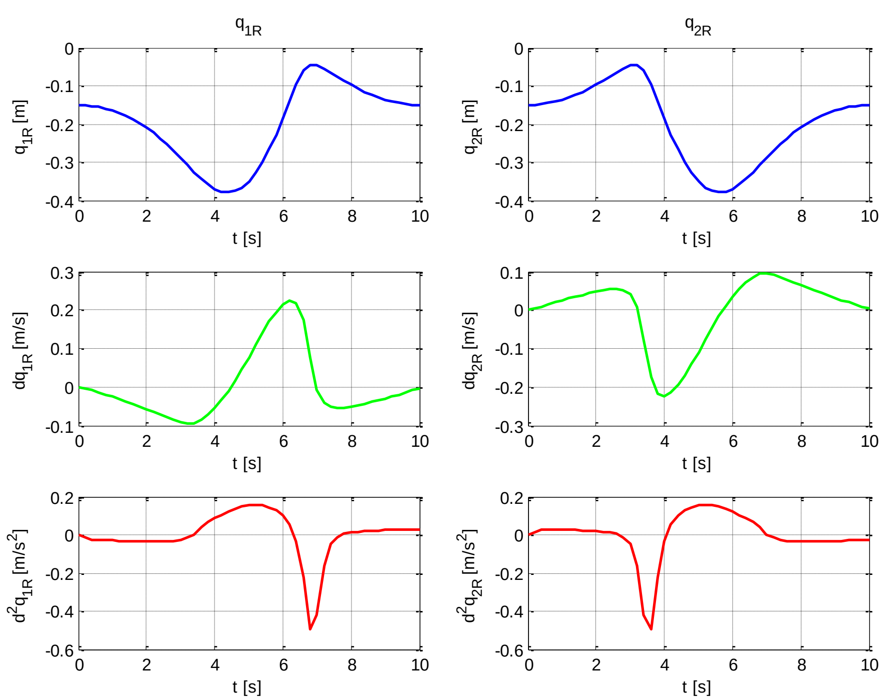

Figure 3.15 Desired/Reference motion law: Joint space

Chapter Four

4. Dynamic modeling and Analysis

The dynamic model of the PRRRP PKM manipulator focuses on analyzing the response motion of the manipulator for a given action of the driving actuator, in this case a pneumatic one. Therefore, this chapter deals with, first, on determining the desired action forces need to be applied by the actuators through an inverse dynamic analysis. Then, it discusses modeling of a pneumatic servo drive in the Matlab/Simulink environment. Finally, it shows how to create a complete dynamic model, analyze the model and discuss the resulting response.

4.1. Dynamic Analysis Approaches

In robotics literature, there are two basic approaches to dynamics, namely Newton-Euler and Lagrangian. For the former, one first carry out a detail force and torque analysis of each rigid link with some physical knowledge such as Newton's third law, and then apply Newton's law and Euler's equation to each of the rigid links to obtain a set of 2nd order Ordinary Differential Equations (ODE) in the position and angular representation of each rigid link. Finally together with the kinematic constraints, the set of equations can be simplified or solved, till the desired form of dynamics equation is obtained. The Lagrangian approach is a more elegant and tractable one which involve the choice of a set of generalize coordinates to describe the configuration of the system, and the setting up of a scalar function called Lagrangian in the tangent bundle of the configuration space.

4.1.1. The Newton-Euler approach

In this approach, first it is necessary to isolate all the rigid links of the system. Then, attach a frame at the center of mass of each rigid link. All the forces and torques applied to each rigid link must be considered. For the forces or torques which are action and reaction pairs are considered to have the same magnitude, opposite directions and act on different bodies along the same line of action according to Newton's third law.

The advantage of this approach is that the formulation is globally valid, i.e. independent of the choice of coordinate system. It is also more intuitive with physical meanings. In literature, there are many variations for the above method, which is basically the difference of a choice of coordinate systems (e.g. body or spatial frame) to describe the various quantities in the systems. In Newton-Euler formulation, in principle, we can account for all the forces and torques applied to each individual link in the systems and derive the equations of motion.[9]

4.1.2. Lagrangian approach

The Lagrangian formulation describes the behavior of a dynamic system in terms of work and energy stored in the system rather than in terms of force and moments of the individual members involved. Using this approach, the closed-form dynamical equations can be derived systematically in any coordinate system. In this paper, Lagrange's equation using constrained coordinates (i.e. the Lagrange multiplier approach) is presented:

$$\frac{d}{dt}\left(\frac{\partial K}{\partial \dot{q}_j}\right) - \frac{\partial K}{\partial q_j} + \frac{\partial U}{\partial q_j} + \sum_{i=1}^{k} \varsigma_i \, G_{ij} = Q_j \,, \; j = 1, \ldots, n,$$

(4.1)

where $\boldsymbol{i}$ is the constraint index, $\boldsymbol{j}$ is the generalized coordinate index, $\boldsymbol{k}$ is the number of constraint functions, $\boldsymbol{K}$ is the total kinetic energy of system, $\boldsymbol{U}$ is the total potential energy term, ς_i is the Lagrange multiplier, $\boldsymbol{G_{ij}}$ is the element of the Jacobian matrix of constraint equation, $\boldsymbol{G_{ij}} = \partial f_i/\partial q_j$, where f_i is a constraint equation, q_j the j^{th} generalized coordinate.

4.2. Inverse Dynamics Analysis through the Newton-Euler approach

The vectors closed-loop of one leg is shown in ***Figure 4.1***. A fixed leg frame B–x'y' is established at the point B and parallel to the global frame O-x y. A local leg frame is also established at the point B while its x-axis is along the leg length direction and its z-axis is parallel to that of the global frame. The vector which represents the inverse kinematic equation of aforementioned closed-loop can be given as

$$r = b + qe_2 + Lw \qquad (4.2)$$

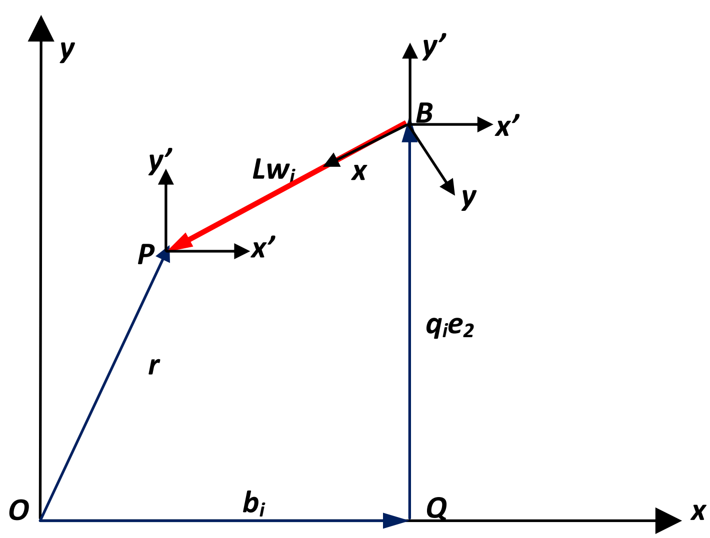

Figure 4.1. Position analysis for a single leg of the PKM manipulator

where $r = [x\ y]^T$ is the position vector of P with respect to the global frame $O\text{-}xy$, $b=[x_B\ 0]^T$ is the position vector of Q with respect to the global frame, and $e_2=[0\ 1]^T$. q is the y coordinate of point B and L and w are the length and unit vector of the leg, respectively, with respect to the global frame. As it is discussed in detail in chapter three, there are four inverse kinematic solutions for a given position of platform. In the configuration shown in ***Figure 3.1***,

$$w = \begin{bmatrix} w_x \\ w_y \end{bmatrix} \tag{4.3}$$

$$w = \begin{bmatrix} \frac{R_1 \pm x}{L_2} \\ \frac{\sqrt{L_2^2 - (R_1 \pm x)^2}}{L_2} \end{bmatrix} \tag{4.4}$$

Where $' \pm '$ in ***Eq. 4.4***, for the configuration shown in ***Figure 3.1***, ' + ' for leg number one and ' - ' for leg number two. Then, the joint position vector q for a single leg can be obtained as:

$$qe_2 = r - b - Lw \tag{4.4}$$

Form the time derivative of ***Eq. 4.2***, the velocity of the joint is obtained as:

$$\dot{r} = \dot{q}e_2 + L\begin{bmatrix} -w_y \\ w_x \end{bmatrix} \tag{4.6}$$

Multiplying both sides of ***Eq. 4.6*** by w^T results in ,

$$\dot{q}w^T e_2 = w^T \dot{r} \tag{4.7}$$

$$\dot{q} = \frac{w^T \dot{r}}{w^T e_2} = \frac{w^T \dot{r}}{w_y} \tag{4.8}$$

Taking the dot product of $[-w_y\ \ w_x]^T$ with both sides of ***Eq. 4.6*** yields in the angular velocity of the leg.

$$\omega = \begin{bmatrix} -w_y \\ w_x \end{bmatrix} \cdot \frac{(\dot{r} - \dot{q}e_2)}{L} \tag{4.9}$$

Further, the time derivative of ***Eq. 4.6*** gives the following equation which, in turn can be rearranged to give a vector of accelerations of the joint, as shown:

$$\ddot{q} = \frac{w^T \ddot{r} + L\omega^2}{w^T e_2} \tag{4.10}$$

Similarly, by taking the dot product of $[-w_y \ \ w_x]^T$ with both sides of ***Eq. 4.10*** the angular acceleration of the leg can be given as:

$$\alpha = \begin{bmatrix} -w_y \\ w_x \end{bmatrix} \cdot \frac{(\ddot{r} - \ddot{q}e_2)}{L} \tag{4.11}$$

Assuming $\boldsymbol{r_c}$ is the position of the centre of gravity of the leg in the local frame $\boldsymbol{B- xy}$, and $\boldsymbol{r'_c}$ is the position of the centre of gravity of the leg with respect to the frame $\boldsymbol{B- x'y'}$, given as:

$$r'_c = \begin{bmatrix} r'_{cx} \\ r'_{cy} \end{bmatrix} = T_c r_c \tag{4.12}$$

Where $T_c$is the rotation matrix from the frame $B- x'y'$ to the frame $B- xy$, and is given by:

$$T_c = \begin{bmatrix} w_x & -w_y \\ w_y & w_x \end{bmatrix} \tag{4.13}$$

Therefore, the position vector of the center of gravity of the leg with respect to the global frame is

$$r_{cg} = b + qe_2 + r'_c \tag{4.14}$$

Taking the time derivative of ***Eq. 4.14*** yields in the velocity of the center of gravity of the leg.

$$\dot{r}_{cg} = \dot{q}e_2 + \omega[-r'_{cy} \quad r'_{cx}]^T \tag{4.15}$$

And, from the time derivative of ***Eq. 4.15***, the acceleration of the center of gravity of the leg can be given as:

$$\ddot{r}_{cg} = \ddot{q}e_2 + \alpha[-r'_{cy} \quad r'_{cx}]^T - \omega^2 r'_c \tag{4.16}$$

4.2.1. The Newton-Euler approach

The objective of this analysis is to obtain the driving forces of actuators, hence, first the force and moment equations of the legs are determined and the constraint forces at the joints are obtained. Then, from the Newton's equation of the carriages, the driving forces of the actuator are finally obtained.

The equation for the dynamic equilibrium of forces applied on the legs can be given by a generalized formula, as shown:

$$F_B + F_P + mg + m\ddot{r}_{cg} = 0 \tag{4.17}$$

Where m is the mass of the leg g is the gravitation acceleration, assuming a horizontal or *X-Y* work table, $g=[0\ 0]^T$. $F_P=[F_{Px}\ \ F_{Py}]^T$ and $F_B=[F_{Bx}\ \ F_{By}]^T$ are the forces exerted on the leg by the end effector and actuator/slider, respectively.

Applying Newton's equation for end effector, yields in:

$$-Mr - \sum_{i=1}^{2} F_{Pi} + F_{ext} + Mg = 0 \tag{4.18}$$

Where M is the mass of the end-effector, and $F_{ext} = [F_x\ F_y]^T$ is the external force exerted on the end-effector.

Besides, the moment equations of a single leg about point *B* are given as :

$$F_P \cdot \begin{bmatrix} -w_y \\ w_x \end{bmatrix} - m\ddot{r}_{cg} \cdot \begin{bmatrix} -r'_{cy} \\ r'_{cx} \end{bmatrix} - mgr'_{cx} - J_B\alpha = 0 \tag{4.19}$$

where $J_B = \frac{1}{3} m_i L_i^2$ is the moment of inertia of the leg to point *B*. Moment equation of the end-effector about point P.

$$M_{ext} - M\ddot{r} \cdot [-R_{cy} \quad R_{cx}]^T = 0 \tag{4.20}$$

Where M_{ext} is the external moment applied on the end-effector and $R_c=[R_{cx}\ R_{cy}]^T$ is the position vector of the center of the end-effector with respect to the frame *P-x'y'*. i.e. $R_c=[0\ 0]$T. Finally, ***Eqs. 4.18, 4.19*** and ***4.20*** are combined into a single linear system of equation in the form shown below.

$$A \begin{bmatrix} F_{P1} \\ F_{P2} \end{bmatrix} = B \tag{4.21}$$

Where,

$$A = \begin{bmatrix} 1 & 0 & 1 & 0 \\ 0 & 1 & 0 & 1 \\ -y & x & -y & x \\ -Lw_{y1} & Lw_{x1} & 0 & 0 \\ 0 & 0 & -Lw_{y2} & Lw_{x2} \end{bmatrix} \quad \text{and} \quad B = \begin{bmatrix} -M\ddot{x} + F_x \\ -M\ddot{y} + F_y + Mg \\ -MgR_{cx} + M_{ext} + M\ddot{x}R_{cy} - M\ddot{y}R_{cx} \\ m_1 gr'_{cx1} + m_1 g\ddot{r}'_{cg1} \cdot \begin{bmatrix} -r'_{cy1} \\ r'_{cx1} \end{bmatrix} + J_{B1}\alpha_1 \\ m_2 gr'_{cx2} + m_2 g\ddot{r}'_{cg2} \cdot \begin{bmatrix} -r'_{cy2} \\ r'_{cx2} \end{bmatrix} + J_{B2}\alpha_2 \end{bmatrix}$$

Then, the solution of ***Eq. 4.21*** yields in the desired forces at point P.

$$[F_{P1}^T \quad F_{P2}^T]^T = A^{-1}B \tag{4.22}$$

The forces exerted on the legs by the sliders at the point B, $F_B=[F_{B1} \;\; F_{B2}]^T$ can be obtained as:

$$F_B = -F_P + m\ddot{r}_{cg} \tag{4.23}$$

From Newton equation applied on the sliders, the driving forces of the actuators can be derived.

The Newton equation for the left actuator:

$$\begin{bmatrix} N_1 \\ F_{d1} \end{bmatrix} + (m_{s1} + m_{a1})g - F_{B1} + f_{bw} - (m_{s1} + m_{a1})\ddot{q}_1 e_2 = 0 \tag{2.24}$$

Similarly, the Newton's equation for the right side actuator:

$$\begin{bmatrix} N_2 \\ F_{d2} \end{bmatrix} + (m_{s2} + m_{a2})g - F_{B2} + f_{bw} - (m_{s2} + m_{a2})\ddot{q}_2 e_2 = 0 \tag{2.25}$$

Where F_{d1} and F_{d2} are the desired drive forces, N_1 and N_2 are reaction forces along the x-axis, m_s and m_a are mass of the slider and actuator, respectively. f_{bw} is the friction force due to actuator-slider interaction. Hence, the drive forces can be extracted from ***Eqs. 2.24*** and ***4.25***:

$$\left.\begin{aligned} F_{d1} &= F_{By1} + (m_{s1} + m_{a1})\ddot{q}_1 - f_{bwy} \\ F_{d2} &= F_{By2} + (m_{s2} + m_{a2})\ddot{q}_2 - f_{bwy} \end{aligned}\right\} \tag{4.26}$$

With the desired drive forces known, the dynamic analysis of the manipulator leads to the next step of modeling a pneumatic actuator which can provide force. Hence, the purpose of the next section would be on modeling a pneumatic drive system that consists of a valve (most probably a proportional directional control valve), a cylinder-piston system and pipe lines and the various connection between them.

4.3. Pneumatic Servo System Modeling

4.3.1. Pneumatic Actuators: Modeling

Several approaches have been proposed for modeling the pneumatic actuators. One of the widely used methods for finding the mathematical model of the pneumatic actuator is a theoretical analysis. The analysis of pneumatic actuators requires a combination of thermodynamics, fluid dynamics and the dynamics of the motion. For constructing a mathematical model, three major considerations must be involved:

1. The determination of the mass flow rates through the valve.
2. The determination of the pressure, volume and temperature of the air in cylinder.
3. The determination of the dynamics of the load.

Accurate model of pneumatic actuator is an important condition both for control design and for optimizing its operation. As a result, this chapter is concerned with the mathematical modeling and numerical simulation for pneumatic actuator systems. [30]

4.3.2. Pneumatic Actuators: The Control Strategies:

The advantages of pneumatic systems are well known as clear, cheap, easily maintained, safe in operation, etc. But for their highly nonlinear properties such as compressibility of medium, friction effect and nonlinearity of valves, pneumatic actuators are seldom used in industrial servo applications. Moreover, some of their properties, e.g., poor damping, low stiffness, and limited bandwidth, are unfavorable in the servo control system design.

Some other difficulties in the control of pneumatic servo systems are the possible presence of unknown disturbances coming from leakage of valves, *time-varying payloads*, and external perturbations. Besides, uncertainties in system parameters make the controller design problem more challenging [30]. To cope with some of these problems, advanced control algorithms have to be proposed.

4.3.3. The Dynamic Model

The dynamic model used in this work is developed based on:

1. the description of the relationship between the air mass flow rate and pressure changes in the cylinder chambers, and
2. the equilibrium of the forces acting at the piston, including the friction force.

A schematic view of the system to be modeled is shown in ***Figure 4.2***.The relationship between the air mass flow rate and the pressure changes in the chambers is obtained using energy conservation laws, and the force equilibrium is given by Newton's second law. The friction force and the external forces are modeled in a unified way.

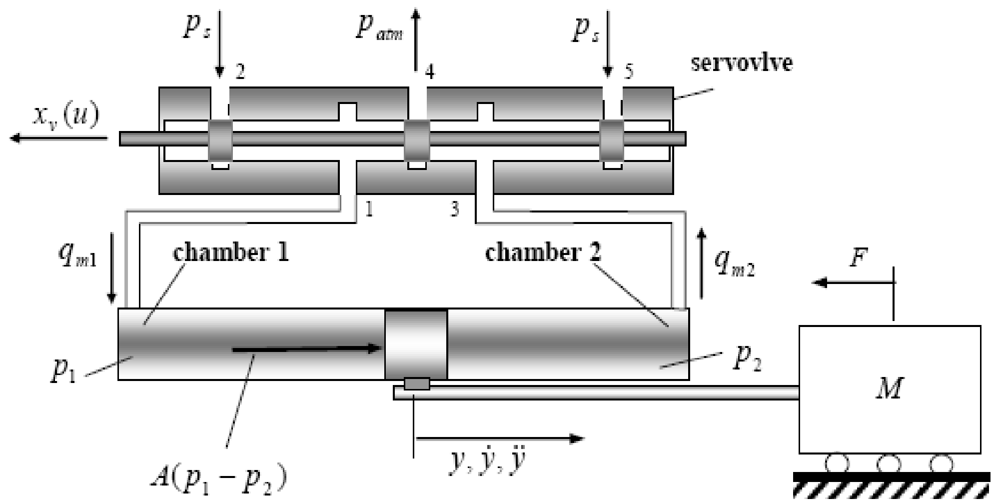

Figure 4.2 Schematic of a Pneumatic Drive System. Source ref. [30]

4.3.3.1. Conservation of Energy

The internal energy of the mass flowing into chamber 1 is $C_p q_{m1} T$, where C_p is the constant pressure specific heat of the air, T is the air supply temperature, and $q_{m1} = \left(\frac{dm}{dt}\right)$ is the air mass flow rate into chamber 1. The rate at which work is done by the moving piston is $p_1 \dot{V}_1$, where p_1 is the absolute pressure in chamber 1 and $\dot{V}_1 = \left(\frac{dV_1}{dt}\right)$ is the volumetric flow rate.

The time air internal energy change rate in the cylinder is $\frac{d(C_V\ \rho_1 V_1 T)}{dt}$, where C_V is the constant volume specific heat of the air and ρ_1 is the air density. We consider the ratio between the specific heat values as $r = C_P / C_V$ and that $\rho_1 = C_V / (RT)$ for an ideal gas, where R is the universal gas constant. An energy balance yields:

$$q_{m1}T - \frac{p_1}{C_P}\frac{dV_1}{dt} = \frac{1}{rR}\frac{d}{dt}(p_1 V_1) \quad (4.27)$$

The total volume of chamber 1 is given by $V_1 = Ay + V_{10}$, where A is the cylinder cross-sectional area, y is the piston position and V_{10} is the dead volume of air in the line and at the chamber 1 extremity. The change rate for this volume is $\dot{V}_1 = A\dot{y}$, where $\dot{y} = \left(\frac{dy}{dt}\right)$ is the piston velocity. After calculating the derivative term in the right hand side of Eq. 4.27, and assuming air is a perfect gas undergoing an isothermal process, the rate of change of the pressure inside each chamber of the cylinder can be expressed as:

$$\dot{p}_1 = -\frac{Ak\dot{y}}{Ay+V_{10}}p_1 + \frac{RkT}{Ay+V_{10}}q_{m1} \tag{4.28}$$

$$\dot{p}_2 = \frac{Ak\dot{y}}{A(L-y)+V_{20}}p_2 + \frac{RkT}{A(L-y)+V_{20}}q_{m2} \tag{4.29}$$

where $C_p = (kR)/(k-1)$ and L is the maximum cylinder stroke. Assuming that the mass flow rates are nonlinear functions of the servovalve control voltage (u) and of the cylinder pressures, that is, $q_{m1} = q_{m1}(p1,u)$ and $q_{m2} = q_{m2}(p2,u)$, ***Eq. 2.28*** and ***Eq. 2.29*** result in,

$$\dot{p}_1 = -\frac{Ak\dot{y}}{Ay+V_{10}}p_1 + \frac{RkT}{Ay+V_{10}}q_{m1}(p_1,u) \tag{4.30}$$

$$\dot{p}_2 = \frac{Ak\dot{y}}{A(L-y)+V_{20}}p_2 + \frac{RkT}{A(L-y)+V_{20}}q_{m2}(p_2,u) \tag{4.31}$$

Therefore, incorporation all the above nonlinear sets of equations, the resulting scheme of the pneumatic drive looks like ***Figure 4.3***, below.

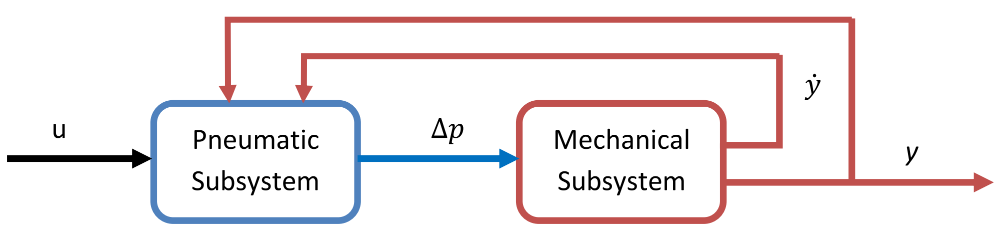

Figure 4.3 Pneumatic drive and mechanical subsystem scheme

Where u is the command signal from the controller/regulator. The Matlab/Simulink model created based on the kinematic and dynamic equations of the PKM manipulator and equations that govern the nonlinear behavior of the pneumatic drive is shown below, in ***Fig. 4.4***.

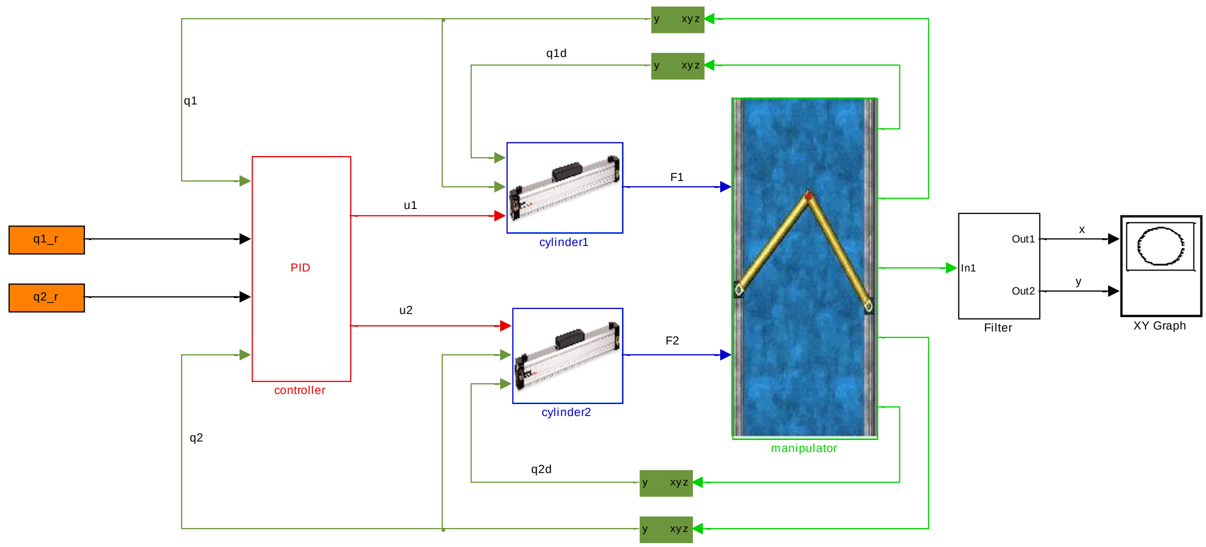

Figure 4.4 Complete dynamic model of the PKM manipulator built in Matlab/Simulink

The detail Matlab code for the dynamic analysis can be found in Appendix-A *part I* by the name of *main_dynamic.m* and *I_dynamic.m*. Also, the detail of the various subsystem blocks in ***Figure 4.4*** are presented in Appendix-A *part II.*

4.4. Simulation results and Discussion

4.4.1. Thermal and physical characteristics of the pneumatic drive

In order to carryout a dynamic numerical simulation the following considerations has been taken.

Table 4.1 Value of Physical and Thermal Constants

Parameter	**Description**
$P_s=6*10^5$ Pa	Cylinder supply pressure
$P_e=1*10^5$ Pa	Cylinder exhaust pressure
$P_a=101.3*10^3$ Pa	Atmospheric pressure
$P_0=3*10^5$ Pa	Initial pressure inside cylinder chambers
$Cr=0.852$	Critical pressure ratio
$T_s=T_c=T_e=293$ K	T_s-Supply air temperature, T_c-cylinder chamber temperature, and T_e-exhaust air temperature. Assuming an isothermal process.
$C1=3.864$	Valve constant
$C2=0.04$	Valve constant
C_p	The constant pressure specific heat of the air
C_V	The constant volume specific heat of the air
$k=1.4$	Heat ratio
$R=287$ $m.K^{-1}$	Gas constant
$B=65$ Nsm^{-1}	Viscous friction coefficient of air
$C_d=0.8$	Valve discharge coefficient

Table 4.2 Pneumatic cylinder characteristics

Model	*FESTO DGP/DGPL*
Size (Bore)	*32 [mm]*
Maximum stroke (Length)	*3000* [mm]*
Base weight	*1550 [g]*
Operating Medium Filtered	*compressed air, unlubricated or lubricated [min. 40 μ]*
Operating Pressure	*2 - 8 [bar]*
Ambient Temperature	*10 to 60 [°C]*

Table 4.3 Proportional valve characteristics

Model	*MPYE Proportional directional control valve*
Valve Function	*5/3-way, normally closed*
Construction design	*Piston spool, directly actuated, controlled spool position*
Sealing principle	*hard*
Actuation type	*Electrical*
Type of rest	*Mechanical spring*
Type of pilot control	*Direct*
Direction of flow	*Non-reversible*
Type of mounting	*Via through-holes*
Mounting position	*any*

4.4.2. Simulink model of pneumatic system

A detailed model of the pneumatic drive system is created, in a Simulink environmet, based on the equations from ***Eq. 4.27*** to ***Eq. 4.31*** and using the data given in ***Tables 4.1, 4.2*** and ***4.3***. The resulting design is shown in ***Figure 4.5***, below.

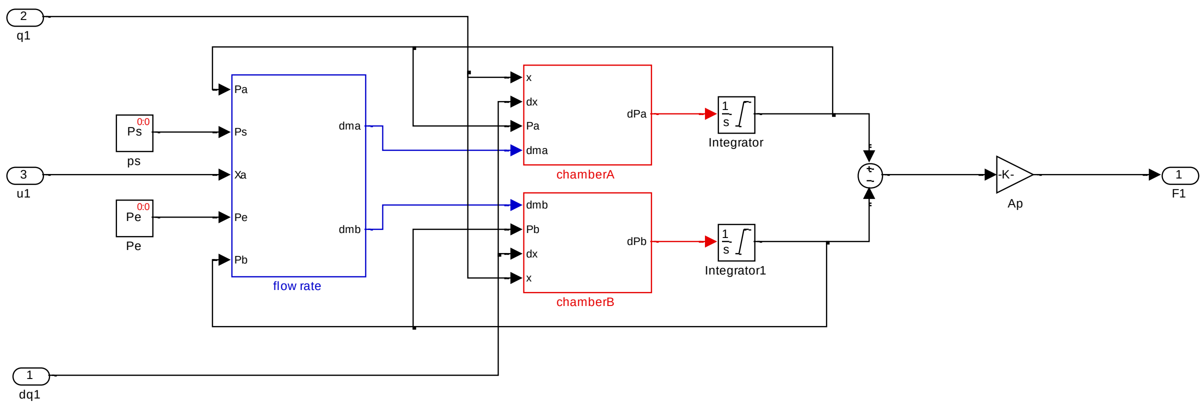

Figure 4.5 Detailed Simulink model of a pneumatic actuator

This subsystems receives a command u, position and speed feedback q and $\dot{q}$, and it gives the change in pressure between chamber A and B. Which then multiplied by the cross-sectional area of the piston A_p and results in the desired force F need to be applied at the manipulators joint.

Chapter Five

5. Control Strategies

The advantages of pneumatic systems are well known such as clear, cheap, easily maintained, safe in operation, etc. But for their highly nonlinear properties such as compressibility of medium, friction effect and nonlinearity of valves, pneumatic actuators are seldom used in industrial servo applications. Moreover, some of their properties, e.g., poor damping, low stiffness, and limited bandwidth, are unfavorable in the servo control system design. Some other difficulties in the control of pneumatic servo systems are the possible presence of unknown disturbances coming from leakage of valves, time-varying payloads, and external perturbations. Besides, uncertainties in system parameters make the controller design problem more challenging.

5.1. A Review of Control strategies

The problem of controlling robots has been extensively important in most of industrial applications. A great variety of control approaches have been proposed throughout the years. The most common which is in use with present industrial robots is a decentralized "proportional, integral, derivative" (PID) control for each degree of freedom. More sophisticated nonlinear control schemes have been developed, such as so-called computed torque control, termed inverse dynamic control, which linearizes and decouples the equation of motion of the robot. In this chapter, first it is discussed the pros and cons PID with respect to other control schemes, i.e. a classical PID control, Sliding mode control, and then the nonlinear linearizing and decoupling control schemes. Then, it focuses on PID controller modeling and tuning based on the need to obtain a good trajectory tracking.

In case of pneumatic drive PID controller is still the most widely used approach due to its ease of implementation, the need for overcoming highly nonlinear phenomena turns away the use of classical PID controllers nowadays, see [4]. Therefore modern control techniques were designed and tested in pneumatic actuators in order to improve the performance of such systems considering position accuracy and repeatability as the two main performance characteristics. Fuzzy logic control, neural networks method, adaptive control, self-tuning or gain scheduling, the so-called "Soft Computing" control techniques, are approaches that have attracted many researchers.

5.1.1. PID Controller

The dynamic model is described by a system of n coupled nonlinear second order differential equations, n being the number of joints. However, for most of today's industrial robots, a local decentralized "proportional, integral, derivative" (PID) control with constant gains is implemented for each joint. The advantages of such a technique are the simplicity of implementation and the low computational cost. The drawbacks are that the dynamic performance of the robot varies according to its configuration, and poor dynamic accuracy when tracking a high velocity trajectory. In many applications, these drawbacks are not of much significance.

The control law is given by:

$$u = K_P\left(q^d - q\right) + K_D\left(\dot{q}^d - \dot{q}\right) + K_I \int_{t0}^{t}\left(q^d - q\right) dt \tag{5.1}$$

Where $e = q^d - q$ is the position error at the joint. The objective function is, then, to get a quality trajectory tracking by minimizing the error in joint position through a compensation of the nonlinearities in the pneumatic drive system.

Practically, the block diagrams of such a control scheme is shown in ***Figure 5.1***.

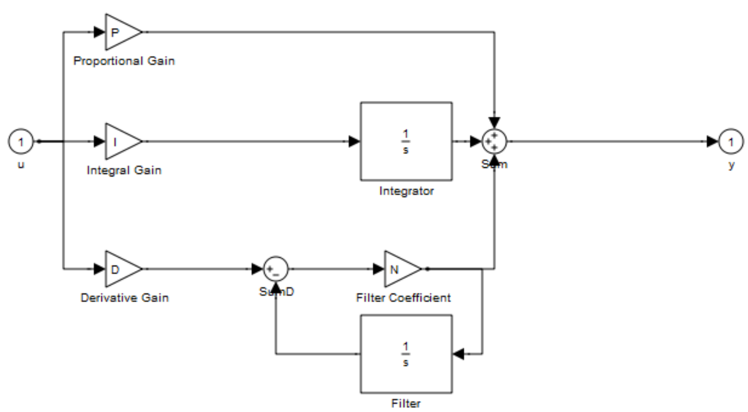

Figure 5.1 PID controller block diagram

5.2. PID Controller Design and tuning

The design is done using a Simulink PID Controller Block , from library: Simulink/Continuous in Matlab. This block takes an error signal and tends to give a tuned value of the gain constants. The PID block is shown in ***Figure 5.2.***

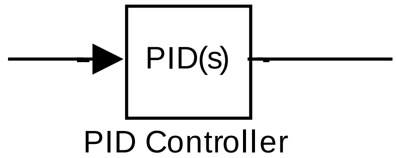

Figure 5.2 PID controller Block in Simulink library

5.2.1. Position Control

As it can be seen from ***Figure 4.4***, the control for trajectory tracking is performed on the joint position. Indirectly, the position of the actuated joints which is also known as the cylinder piston displacement is compared with the desired joint position.

To be Continued …

Conclusions

The objective of this thesis work was to carry out a full kinematic and dynamic analysis of a 2 DoF planar PKM manipulator driven by a pneumatic actuator. Thereby, to devise an appropriate control strategy in order to eliminate the position error that might be induced due to the nonlinearity in the drive mechanism.

Accordingly, in third chapter, it is presented detailed kinematic analysis. The model used in the kinematic simulation is designed in a Matlab/Simulink environment and it includes a physical representation of the manipulator created in Solidworks interface and then translated into a Simmechanics equivalent. The response of the manipulator for a desired input trajectory, in this case a circle under the effective work-envelop and desired motion law, i.e. a symmetric constant acceleration law, was as expected. Means, there isn't position error due to only the kinematic of the mechanism because, it has been assumed that all the linkages in the PKM manipulator are rigid.

Whereas, as it is presented in the subsequent chapters, four and five, it has been tried to make a full dynamic analysis, which includes modeling of a pneumatic drive in a Matlab/Simulink environment. A model of the pneumatic actuator is created, as it is stated in chapter four, based on a set of nonlinear state flow and thermal equations. However, at the end of the analysis it appears to have a problem on the control of the resulting response. i.e. the manipulator very hardly follows the desired circular trajectory. As a result, I have faced difficulties on designing a control scheme that can compensate this huge gap in position.

Having spent too much effort and time on finding/creating a pneumatic actuator model that may result in a reasonable response, I still couldn't overcome this difficulty. Therefore, due to lack of additional time, my limited scope of knowledge on pneumatics and also the economic situation I am in now, I am forced to compile the unfinished work that I have done so far. Which I hope leads me to my graduation.

Appendix A

1. Part I - Program Details

Detail of the Matlab Code Written for Inverse Kinematic Analysis
main_kinematic.m

```
%%%%%%%%%%%%%%%%%%%%%%%%%%%%%%%%%%%%%%%%%%%%%%%%%%%%%%%%%%%%%%%%%%%%%%%%%%%
%Master's Thesis
%Title: Dynamic Analysis of a Planar Manipulator Driven by Pneumatic
%Actuators
%By:Mhreite Moalign Mulusew
%Supervisors: Eng Hermes Giberti and Ing Simone Cinquemanii
%%%%%%%%%%%%%%%%%%%%%%%%%%%%%%%%%%%%%%%%%%%%%%%%%%%%%%%%%%%%%%%%%%%%%%%%%%%
%NOTE: This Matlab program is written for the kinematic analysis of the
%manipulator. To be fully functional, this program requires the following
%Matalb and Simulink files: 1) Constant_Acceleration_ND.m
%                            2) sim_kinematics.mdl
%All the above files should be placed in same folder(directory) that
%contains this main program.
%%%%%%%%%%%%%%%%%%%%%%%%%%%%%%%%%%%%%%%%%%%%%%%%%%%%%%%%%%%%%%%%%%%%%%%%%%%
clear all
close all
clc

%Robot geometric parameters
l1=0.500;       %Horizontal distance between the two sliders/actuators [m]
l2=0.354;       %Length of a single arm [m]
l3=1.500;       %Maximum length of actuator [m]
R1=l1/2;
R2=l2;

T=10;               %Simulation time[s]
t=0:0.1:T;
%%-------------------------------------------------------------------------
%%
%Desired trajectory
%Circle
Rc=0.1;             %Radius of the circle[m]
angle=2*pi;         %Total angle covered by a circle angle[rad]
angle_0=0;          %Angle corresponding to initial position [rad]
%%-------------------------------------------------------------------------
%%
%Initial conditions of the manipulator
    xc=0;                   %x_position of the center of the circle [m]
    yc=-0.0790919;          %y_position of the center of the circle [m]
    Dangle=angle-angle_0;
    Xo=xc+Rc;               %Initial x-position of the end effector [m]
    Yo=yc;                  %Initial y-position of the end effector [m]
    vXo=0;                  %Initial velocity of the manipulator  in x-
axis[m/s]
    vYo=0;                  %Initial velocity of the manipulator in y-
axis[m/s]
%%-------------------------------------------------------------------------
%%
```

```
% Motion law of the End-Effector (Constant Acceleratin Law)
ndt=t./T;
par=[1/3,1/3];

[D,V,A] = Constant_Acceleration_ND(ndt,par);

    theta=Dangle*D;
    thetaD=Dangle/T*V;
    thetaDD=Dangle/T^2*A;

    xx=Rc*sin(theta);
    yy=Rc*(cos(theta));
    xd=Rc*thetaD.*cos(theta);
    yd=Rc*thetaD.*sin(theta);
    xdd=Rc*(thetaDD.*cos(theta)-(thetaD.^2).*sin(theta));
    ydd=Rc*(thetaDD.*sin(theta)+(thetaD.^2).*cos(theta));
 %%--------------------------------------------------------------------------
 %%
 %%PLOT OF THE DESIRED TRAJECTORY
        figure('Number','Off','Name','DESIRED TRAJECTORY')
         plot(xx,yy);grid on;axis equal
%%---------------------------------------------------------------------------
%%
%%END EFFECTOR DESIRED MOTION LAW
figure('Number','Off','Name','END-EFFECTOR DESIRED MOTION LAW [SYMMETRIC
CONSTANT ACCELERATION LAW')
 subplot(311);
 plot(t,theta,'LineWidth',2);grid on;xlabel('t [s]');ylabel('theta [rad]')
 subplot(312)
 plot(t,thetaD,'g','LineWidth',2); grid on;xlabel('t [s]');ylabel('d(theta)
[rad/s]')
 subplot(313)
 plot(t,thetaDD,'r','LineWidth',2); grid on;xlabel('t
[s]');ylabel('d^2(theta) [rad/s^2]')
 %%--------------------------------------------------------------------------
 %%
 %%END EFFECTOR DESIRED MOTION LAW DECOMPOSED FOR THE X-AXIS AND Y-AXIS
figure('Number','Off','Name','END-EFFECTOR DESIRED MOTION LAW [DECOMPOSED
TO X & Y AXES]')
 subplot(321);
 plot(t,xx,'LineWidth',2); title('Axis-X');grid on;xlabel('t
[s]');ylabel('X [m]')
 subplot(323)
 plot(t,xd,'g','LineWidth',2); grid on;xlabel('t [s]');ylabel('dX [m/s]')
 subplot(325)
 plot(t,xdd,'r','LineWidth',2); grid on;xlabel('t [s]');ylabel('d^2X
[m/s^2]')

 subplot(322);
 plot(t,yy,'LineWidth',2); title('Axis-Y');grid on; xlabel('t
[s]');ylabel('X [m]')
 subplot(324)
 plot(t,yd,'g','LineWidth',2); grid on;xlabel('t [s]');ylabel('dX [m/s]')
 subplot(326)
 plot(t,ydd,'r','LineWidth',2); grid on;xlabel('t [s]');ylabel('d^2X
[m/s^2]')
 %%--------------------------------------------------------------------------
```

```
 %%
 %INVERSE KINEMATIC ANALYSIS

%joint space position
    q1=yy - sqrt(R2^2 -(xx + R1).^2);
    q2=yy - sqrt(R2^2 -(xx - R1).^2);
    Q=[q1;q2];

for i=1:length(t)
%Jacobiam matrix
    J=[(xx(i)-R1)/sqrt(R2^2-(xx(i)-R1).^2)  1;
       (xx(i)+R1)/sqrt(R2^2-(xx(i)+R1).^2)  1];

%Joint space velocity
    Qd(:,i)=J*[xd(i);yd(i)];
    q1d=Qd(1,:);
    q2d=Qd(2,:);

%Matrix A(p,pd)
    A_A=[(xx(i)^2 + yy(i)^2 - 2*yd(i)*Qd(1) + Qd(1).^2)/(yy(i) - q1(i));
         (xx(i)^2 + yy(i)^2 - 2*yd(i)*Qd(2) + Qd(2).^2)/(yy(i) - q2(i))];

%Joint space acceleration
    Qdd(:,i)=J*[xdd(i);ydd(i)] + A_A;

end
q1dd=Qdd(1,:);
q2dd=Qdd(2,:);

%%---------------------------------------------------------------------------
 %%
 %%DESIRED MOTION LOW IN THE JOINT SPACE. MATLAB BASED ANALYSIS
figure('Number','Off','Name','REFERENCE MOTION LAW [ JOINT SPACE ]_MATLAB')
 subplot(321);
 plot(t,q1); title('q_1_R');grid on;xlabel('t [s]');ylabel('q_1_R [m]')
 subplot(323)
 plot(t,Qd(1,:),'g'); grid on;xlabel('t [s]');ylabel('dq_1_R [m/s]')
 subplot(325)
 plot(t,Qdd(1,:),'r'); grid on;xlabel('t [s]');ylabel('d^2q_1_R [m/s^2]')

 subplot(322);
 plot(t,q2); title('q_2_R');grid on; xlabel('t [s]');ylabel('q_2_R [m]')
 subplot(324)
 plot(t,Qd(2,:),'g'); grid on;xlabel('t [s]');ylabel('dq_2_R [m/s]')
 subplot(326)
 plot(t,Qdd(2,:),'r'); grid on;xlabel('t [s]');ylabel('d^2q_2_R [m/s^2]')
 %%--------------------------------------------------------------------------
 %%
 %%VARIABLES THAT CAN BE USED IN SIMULINK AS AN INPUT
    xx_r=[t;xx]';
    yy_r=[t;yy]';
    q1_r=[t;q1]';
    q2_r=[t;q2]';
    q1d_r=[t;Qd(1,:)]';
    q2d_r=[t;Qd(2,:)]';
    q1dd_r=[t;Qdd(1,:)]';
```

```
   q2dd_r=[t;Qdd(2,:)]';
 %%-----------------------------------------------------------------------
 %%
 %%SIMULINK BASED KINEMATIC ANALYSIS
 open('sim_kinematic.mdl')
 sim('sim_kinematic')
   xp=x.signals.values;
   yp=y.signals.values;
   xr=x_r.signals.values;
   yr=y_r.signals.values;
   tt=x.time;
   q1_=q1_r1.signals.values;
   q2_=q2_r1.signals.values;
   q1d=q1dot_r.signals.values;
   q2d=q2dot_r.signals.values;
   q1dd=q12dot_r.signals.values;
   q2dd=q22dot_r.signals.values;
%%------------------------------------------------------------------------
%%
%%DESIRED MOTION LAW IN THE JOINT SPACE. SIMULINK BASED ANALYSIS
figure('Number','Off','Name','REFERENCE MOTION LAW [ JOINT SPACE
]_SIMULINK')
 subplot(321);
 plot(tt,q1_,'LineWidth',2); title('q_1_R');grid on;xlabel('t
[s]');ylabel('q_1_R [m]')
 subplot(323)
 plot(tt,q1d,'g','LineWidth',2); grid on;xlabel('t [s]');ylabel('dq_1_R
[m/s]')
 subplot(325)
 plot(tt,q1dd,'r','LineWidth',2); grid on;xlabel('t [s]');ylabel('d^2q_1_R
[m/s^2]')

 subplot(322);
 plot(tt,q2_,'LineWidth',2); title('q_2_R');grid on; xlabel('t
[s]');ylabel('q_2_R [m]')
 subplot(324)
 plot(tt,q2d,'g','LineWidth',2); grid on;xlabel('t [s]');ylabel('dq_2_R
[m/s]')
 subplot(326)
 plot(tt,q2dd,'r','LineWidth',2); grid on;xlabel('t [s]');ylabel('d^2q_2_R
[m/s^2]')
 %%-----------------------------------------------------------------------
 %%
 %%TRAJECTORY COMPARISON AND POSITION ERROR ANALYSIS
figure('Number','Off','Name','TRAJECTORY COMPARISON...KINEMATIC ANALYSIS')
  hold on
  plot(xr,yr);grid on
  plot(xp,yp,'r');grid on
  axis equal

  ex=xr-xp;
  ey=yr-yp;

figure('Number','Off','Name','End-effector Position Error in the X-axis &
Y-axis')
  subplot(2,1,1);
  plot(tt,ex),ylim([-2 2]);title('Error along x-axis');grid on;
```

```
  subplot(2,1,2);
  plot(tt,ey,'r'),ylim([-2 2]);title('Error along y-axis');grid on;

%%--------------------------E--N--D---------------------------------------
```

Detail of the Matlab Code Written for a Symmetric Constant Acceleration Law
Constant_Acceleration_ND.m

```
%%%%%%%%%%%%%%%%%%%%%%%%%%%%%%%%%%%%%%%%%%%%%%%%%%%%%%%%%%%%%%%%%%%%%%%%%%%%
%Master's Thesis
%Title: Dynamic Analysis of a Planar Manipulator Driven by Pneumatic
%Actuators
%By:Mhretie Moalign Mulusew
%Supervisors: Eng Hermes Giberti and Ing Simone Cinquemanii
%%%%%%%%%%%%%%%%%%%%%%%%%%%%%%%%%%%%%%%%%%%%%%%%%%%%%%%%%%%%%%%%%%%%%%%%%%%%
%NOTE: This Matlab Function is written for generating a Symmetric Constant
%Acceleration Law.
%%%%%%%%%%%%%%%%%%%%%%%%%%%%%%%%%%%%%%%%%%%%%%%%%%%%%%%%%%%%%%%%%%%%%%%%%%%%

 function [D,V,A] = Constant_Acceleration_ND(x,par)

% Non-dimensional General Constant Acceleration Motion Law
%
% x = t/tm non-dimensional time
% D = non-dimensional displacement
% V = non-dimensional velocity
% A = non-dimensional acceleration
% par(1) = xa+
% par(2) = xa-
%par=[1/3,1/3];

xap = par(1); %Positive acceleration part
xam = par(2); %Negative acceleration part

cap = 1/(xap*(1-(xap+xam)/2));
cam = 1/(xam*(1-(xap+xam)/2));

for i=1:length(x)

  if x(i)>=0 && x(i)<=xap
   A(i)=cap;
   V(i)=cap*x(i);
   D(i)=0.5*cap*x(i)^2;
  end
  if x(i)>xap && x(i)<(1-xam)
   A(i)=0;
   V(i)=cap*xap;
   D(i)=cap*xap*(x(i)-xap/2);
  end
  if x(i)>=(1-xam) && x(i)<=1
   A(i)=-cam;
   V(i)=cap*xap-cam*(x(i)-1+xam);
   D(i)=cap*xap*(x(i)-xap/2)-cam/2*(x(i)-1+xam)^2;
  end
end
%%--------------------------E--N--D---------------------------------------
```

Detail of the Matlab Code Written for Direct Kinematic Analysis
D_kinematic.m

```
%%%%%%%%%%%%%%%%%%%%%%%%%%%%%%%%%%%%%%%%%%%%%%%%%%%%%%%%%%%%%%%%%%%%%%%%%%%%%
%

%Master's Thesis
%Title: Dynamic Analysis of a Planar Manipulator Driven by Pneumatic
%Actuators
%By:Mhretie Moalign Mulusew
%Supervisors: Eng Hermes Giberti and Ing Simone Cinquemanii

%%%%%%%%%%%%%%%%%%%%%%%%%%%%%%%%%%%%%%%%%%%%%%%%%%%%%%%%%%%%%%%%%%%%%%%%%%%%%
%NOTE: This Matlab Function is written for a Direct Kinematics
%%%%%%%%%%%%%%%%%%%%%%%%%%%%%%%%%%%%%%%%%%%%%%%%%%%%%%%%%%%%%%%%%%%%%%%%%%%%%

function [PP]=D_kinematic(Q1,Q2)

global R1 R2 t

 for i=1:(length(t))
q1=Q1(i);
q2=Q2(i);

a=(q2 - q1)/(2*R1);
b=(q1^2 - q2^2)/(4*R1);
e=a^2 + 1;
g=(b-R1)^2 + q1^2 - R2^2;
f=2*a*(b - R1) - q1*2;

y(i)=-(f - sqrt(f^2 - 4*e*g))/(2*e);
x(i)=a*y(i)+b;
 end

PP=[x;y];
%%------------------------------E--N--D-----------------------------------
```

Detail of the Matlab Code Written for Workspace Generation
Workspace.m

```
%%%%%%%%%%%%%%%%%%%%%%%%%%%%%%%%%%%%%%%%%%%%%%%%%%%%%%%%%%%%%%%%%%%%%%%%%%%%%
%NOTE: This Matlab Function is written for generating Workspace Envelop
%%%%%%%%%%%%%%%%%%%%%%%%%%%%%%%%%%%%%%%%%%%%%%%%%%%%%%%%%%%%%%%%%%%%%%%%%%%%%

close all
clear all
clc

%Input parameters
l1=0.500; %mm
l2=0.354; %mm
l3=1.500;%mm
R1=l1/2;
```

```
R2=l2;

%%workspace
q=0:0.1:1.25;
for i=1:length(q)
    q1=q(i);
    for j=1:length(q)
        q2=q(j);
        Q=[q1;q2];
        [x,y]=D_kinematic(Q);
 plot(x,y,'*')
 hold on
 title('Workspace')
 axis([-0.25,0.25,0,1.5])
    end
end
%%--------------------------E--N--D----------------------------------------
```

Detail of the Matlab Code Written for Dynamic Analysis

main_dynamic.m

```
%%%%%%%%%%%%%%%%%%%%%%%%%%%%%%%%%%%%%%%%%%%%%%%%%%%%%%%%%%%%%%%%%%%%%%%%%%%
%Master's Thesis
%Title: Dynamic Analysis of a Planar Manipulator Driven by Pneumatic
%Actuators
%By:Mhretie Moalign Mulusew
%Supervisors: Eng Hermes Giberti and Ing Simone Cinquemanii
%%%%%%%%%%%%%%%%%%%%%%%%%%%%%%%%%%%%%%%%%%%%%%%%%%%%%%%%%%%%%%%%%%%%%%%%%%
%NOTE: This Matlab program is written for the dynamic analysis of the
%manipulator. To be fully functional, this program requires the following
%Matalb and Simulink files: 1) Constant_Acceleration_ND.m
%                           2) Inverse_Dynamics.m , and
%                           3) sim_dynamics.mdl
%All the above files should be placed in same folder(directory) that
%contains this main program.
%%%%%%%%%%%%%%%%%%%%%%%%%%%%%%%%%%%%%%%%%%%%%%%%%%%%%%%%%%%%%%%%%%%%%%%%%%%
clear all
close all
clc

global l1 l2 R1 J1 J2 M m1 m2 ms mcy g

%Robot geometric parameters
l1=0.500;       %Horizontal distance bteween the two sliders/actuators [m]
l2=0.354;       %Length of a single arm [m]
l3=1.500;       %Maximum length of actuator [m]

%Physical and Thermal Constants
Ps=6e5;         %Cylinder Supply pressure [Pa]
Pe=1e5;         %Cylinder Exhaust pressure [Pa]
P0=3e5;         %Initial pressure in the cylinder [Pa]
Patm=101.3e3;   %average atmospheric pressure [Pa]
Cr=0.852;       %Critical pressure ratio[]
Ts=293;         %Supply temperature [K]
```

```
Tc=Ts;           %Cylinder temperature [K]...Isothermal process
Tp=Ts;           %Pipe temperature [K]...Isothermal process
Ck=3.864;        %Valve constant1[]
Co=0.04;         %Valve constant2[]
Cd=0.8;          %valve coeffiecent of discharger[]
Cs=Cd;
Cc=0.7;          %Connection port discharge coefficient []
Cv=3.15745e-4;   %Valve constant[m/V]
B=65;            %Viscous friction coefficient of air[Ns/m]
k=1.4;           %Heat ratio
gam=k;
R=287;           %Gas constant [m/K]
g=0;             %Gravitational Acceleration [m/s^2]
ms=1;            %Mass of slider [kg]
mcy=1;           %Mass of Cylinder piston [kg]
m1=2;            %Mass of leg one [kg]
m2=2;            %Mass of leg two [kg]
M=5;             %Mass of end-effector [kg]

Wa=5e-3;         %valve opening width for intake valve [m]
Wb=5e-3;         %valve opening width for exhaust valve[m]
dp=0.016;        %Cylinder bore or Piston diameter [m]
L=1.5;           %Cylinder length [m]

%Calculated geometric parameters related to actuator
Ap=pi*dp^2;          %Cylinder area or piston cross-sectional area [m^2]
Acy=Ap;
Vc=L*Ap;             %cylinder volume [m^3]
Vp=0.5*pi*0.02^2;    %Pipe effective volume [m^3]

%Calculated robot geometric parametrs
R1=l1/2;
R2=l2;
J1=(1/3)*m1*l2^3;     %Moment of inertia of leg #one about point B1 [kg m^3]
J2=(1/3)*m2*l2^3;     %Moment of inertia of leg #two about point B1 [kg m^3]

%Control Parameters
Kp=1;                %Proportional gain []
Ki=0;                %Integral gain []
Kd=0;                %derivative gain []

T=10;                %Simulation time[s]
t=0:0.1:T;

%%-------------------------------------------------------------------------
%%
%Desired trajectory
%Circle
Rc=0.1;              %Radius of the circle[m]
angle=2*pi;          %Total angle covered by a circle angle[rad]
angle_0=0;           %Angle corresponding to initial position [rad]
%%-------------------------------------------------------------------------
%%
%Initial conditions of the manipulator

    xc=0;                    %x_position of the center of the circle [m]
```

```
    yc=-0.0790919;          %y_position of the center of the circle [m]
    Dangle=angle-angle_0;
    Xo=xc+Rc;               %Initial x-position of the end effector [m]
    Yo=yc;                  %Initial y-position of the end effector [m]
    vXo=0;                  %Initial velocity of the manipulator along x-
axis[m/s].... considering that the robot start from rest
    vYo=0;                  %Initial velocity of the manipulator along y-
axis[m/s].... considering that the robot start from rest

%     q10=-0.0840919;          %Yo - sqrt(R2^2 -(Xo - R1)^2);
%     q20=-0.0840919;          %Yo - sqrt(R2^2 -(Xo + R1)^2);
%%---------------------------------------------------------------------------
%%
% Motion law of the End-Effector (Constant Acceleratin Law)

ndt=t./T;
par=[1/3,1/3];

[D,V,A] = Constant_Acceleration_ND(ndt,par);

    theta=Dangle*D;
    thetaD=Dangle/T*V;
    thetaDD=Dangle/T^2*A;

    xx=Rc*sin(theta);
    yy=Rc*(cos(theta));

    xd=Rc*thetaD.*cos(theta);
    yd=Rc*thetaD.*sin(theta);

    xdd=Rc*(thetaDD.*cos(theta)-(thetaD.^2).*sin(theta));
    ydd=Rc*(thetaDD.*sin(theta)+(thetaD.^2).*cos(theta));
 %%--------------------------------------------------------------------------
 %%
 %%PLOT OF THE DESIRED TRAJECTORY
    figure('Number','Off','Name','DESIRED TRAJECTORY')
         plot(xx,yy);grid on;axis equal
%%---------------------------------------------------------------------------
%%
%%PLOT OF THE DESIRED MOTION LAW

figure('Number','Off','Name','END-EFFECTOR DESIRED MOTION LAW [SYMMETRIC
CONSTANT ACCELERATION LAW')
subplot(311);
plot(t,theta);grid on;xlabel('t [s]');ylabel('theta [rad]')
subplot(312)
plot(t,thetaD,'g'); grid on;xlabel('t [s]');ylabel('d(theta) [rad/s]')
subplot(313)
plot(t,thetaDD,'r'); grid on;xlabel('t [s]');ylabel('d^2(theta) [rad/s^2]')
 %%--------------------------------------------------------------------------
 %%
 %%PLOT OF THE DESIRED MOTION OF THE END EFFECTOR

    figure('Number','Off','Name','END-EFFECTOR DESIRED MOTION LAW
[DECOMPOSED TO X & Y AXES]')
         subplot(321);
```

```
            plot(t,xx); title('Axis-X');grid on;xlabel('t [s]');ylabel('X
[m]')
         subplot(323)
            plot(t,xd,'g'); grid on;xlabel('t [s]');ylabel('dX [m/s]')
         subplot(325)
            plot(t,xdd,'r'); grid on;xlabel('t [s]');ylabel('d^2X [m/s^2]')

         subplot(322);
            plot(t,yy); title('Axis-Y');grid on; xlabel('t [s]');ylabel('X
[m]')
         subplot(324)
            plot(t,yd,'g'); grid on;xlabel('t [s]');ylabel('dX [m/s]')
         subplot(326)
            plot(t,ydd,'r'); grid on;xlabel('t [s]');ylabel('d^2X [m/s^2]')
 %%-----------------------------------------------------------------------
 %%
 %INVERSE KINEMATIC ANALYSIS
%Joint space position
    q1=yy - sqrt(R2^2 -(xx + R1).^2);   %considering only one(+)solution
out of the four possible results
    q2=yy - sqrt(R2^2 -(xx - R1).^2);   %based on the configuration
discussed in the third chapter of the report
    Q=[q1;q2];

for i=1:length(t)
 %Jacobian matrix

    J=[-(xx(i)-R1)/sqrt(R2^2-(xx(i)-R1).^2)  1;
       -(xx(i)+R1)/sqrt(R2^2-(xx(i)+R1).^2)  1];

%Joint space velocity
    Qd(:,i)=J*[xd(i) yd(i)]';

%Matrix A(p,pd)
    A_A=[(xx(i)^2 + yy(i)^2 - 2*yd(i)*Qd(1) + Qd(1).^2)/(yy(i) - q1(i));
         (xx(i)^2 + yy(i)^2 - 2*yd(i)*Qd(2) + Qd(2).^2)/(yy(i) - q2(i))];

%Joint space acceleration
    Qdd(:,i)=J*[xdd(i);ydd(i)] + A_A;

 end
    q1d=Qd(1,:);
    q2d=Qd(2,:);
    q1dd=Qdd(1,:);
    q2dd=Qdd(2,:);
 %%------------------------------------------------------------------------
 %%
 %%PLOTS OF JOINT SPACE MOTION (POSITION, VELOCITY & ACCELERATION)

figure('Number','Off','Name','REFERENCE MOTION LAW [ JOINT SPACE ]')
 subplot(321);
     plot(t,q1); title('q_1_R');grid on;xlabel('t [s]');ylabel('q_1_R [m]')
 subplot(323)
     plot(t,q1d,'g'); grid on;xlabel('t [s]');ylabel('dq_1_R [m/s]')
 subplot(325)
     plot(t,q1dd,'r'); grid on;xlabel('t [s]');ylabel('d^2q_1_R [m/s^2]')
```

```
 subplot(322);
    plot(t,q2); title('q_2_R');grid on; xlabel('t [s]');ylabel('q_2_R [m]')
 subplot(324)
    plot(t,q2d,'g'); grid on;xlabel('t [s]');ylabel('dq_2_R [m/s]')
 subplot(326)
    plot(t,q2dd,'r'); grid on;xlabel('t [s]');ylabel('d^2q_2_R [m/s^2]')
 %%------------------------------------------------------------------------
 %%
 %%INVERSE DYNAMIC ANALYSIS
  [FB1 FB2 Fd1 Fd2]=Inverse_Dynamics(t,xx,yy,xd,yd,xdd,ydd);

 %%------------------------------------------------------------------------
 %%
 %%PLOTS OF DESIRED DRIVE FORCES
  figure('Number','Off','Name','Desired Force at Slider Joint 1')
 subplot(211)
 plot(t,FB1(1,:));title('X-axis component');xlabel('t [s]');ylabel('F
[N]');grid on
 subplot(212)
    plot(t,FB1(2,:));title('Y-axis component');xlabel('t [s]');ylabel('F
[N]');grid on

 figure('Number','Off','Name','Desired Force at Slider Joint 2')
     subplot(211)
        plot(t,FB2(1,:));title('X-axis component');xlabel('t
[s]');ylabel('F [N]');grid on
     subplot(212)
        plot(t,FB2(2,:));title('Y-axis component');xlabel('t
[s]');ylabel('F [N]');grid on

 figure('Number','Off','Name','Desired Drive Force')
     subplot(211)
        plot(t,Fd1);title('Drive Force at Slider Joint#1');xlabel('t
[s]');ylabel('F_d_1 [N]');grid on
     subplot(212)
        plot(t,Fd2);title('Drive Force at Slider Joint#2');xlabel('t
[s]');ylabel('F_d_2 [N]');grid on
  %%-----------------------------------------------------------------------
  %%
  %VARIABLE USED AS AN INPUT TO THE SIMULINK MODELS
    xx_r=[t;xx]';
    yy_r=[t;yy]';
    q1_r=[t;q1]';
    q2_r=[t;q2]';
    q1d_r=[t;Qd(1,:)]';
    q2d_r=[t;Qd(2,:)]';
    q1dd_r=[t;Qdd(1,:)]';
    q2dd_r=[t;Qdd(2,:)]';
    F1_r=[t;Fd1]';
    F2_r=[t;Fd2]';
 %%------------------------------E--N--d---------------------------------%%
```

This Matlab Code is Written for Inverse Dynamic Analysis using Newton-Euler Approach

I_Dynamic.m

```
%%%%%%%%%%%%%%%%%%%%%%%%%%%%%%%%%%%%%%%%%%%%%%%%%%%%%%%%%%%%%%%%%%%%%%%%%%%
%Master's Thesis
%Title: Dynamic Analysis of a Planar Manipulator Driven by Pneumatic
%Actuators
%By:Mhretie Moalign Mulusew
%Supervisors: Eng Hermes Giberti and Ing Simone Cinquemanii
%%%%%%%%%%%%%%%%%%%%%%%%%%%%%%%%%%%%%%%%%%%%%%%%%%%%%%%%%%%%%%%%%%%%%%%%%%%
%NOTE: This Matlab Function is written for Inverse Dynamic Analysis using
%the Newton-Euler Approach
%%%%%%%%%%%%%%%%%%%%%%%%%%%%%%%%%%%%%%%%%%%%%%%%%%%%%%%%%%%%%%%%%%%%%%%%%%%

function[FB1 FB2 Fd1 Fd2]=Inverse_Dynamics(t,xx_,yy_,xd_,yd_,xdd_,ydd_)

global l1 l2 R1 J1 J2 M m1 m2 ms mcy g
l=l2;
Rcg=l2/2;

for i=1:length(t);
    xx=xx_(:,i);
    yy=yy_(:,i);
    xd=xd_(:,i);
    yd=yd_(:,i);
    xdd=xdd_(:,i);
    ydd=ydd_(:,i);
r=[xx yy]';
rd=[xd yd]';
rdd=[xdd ydd]';
Rc=[Rcg 0]';
a=[0 0]';
e2=[0 1]';
b=[l1/2 0]';

lx1=R1+r(1);
lx2=R1-r(1);
w1=(1/l2)*[lx1  sqrt(l2^2-lx1^2)]';
w2=(1/l2)*[lx2  sqrt(l2^2-lx2^2)]';

%%velocity Analysis
q1d=(w1'*rd)/w1(2);
q2d=(w2'*rd)/w2(2);

rqd1=rd-q1d*e2;
omega1=(1/l2)*(-w1(2)*rqd1(1)+w1(1)*rqd1(2));
rqd2=rd-q2d*e2;
omega2=(1/l2)*(-w2(2)*rqd2(1)+w2(1)*rqd2(2));

%%Acceleration Analysis
q1dd=(1/w1(2))*(w1'*rdd + l*(omega1^2));
q2dd=(1/w2(2))*(w2'*rdd + l*(omega2^2));

rqdd1=rdd-q1dd*e2;
alfa1=(1/l2)*(-w1(2)*rqdd1(1)+w1(1)*rqdd1(2));
rqdd2=rdd-q2dd*e2;
```

```
alfa2=(1/l2)*(-w2(2)*rqdd2(1)+w2(1)*rqdd2(2));

%%--------------------------------------------------------------------------
%%
%%Postion,Velocity and Acceleration analysis at the center of gravity of
legs
%Position
Tc1=[w1(1) -w1(2);
     w1(2) w1(1)];

Rc1_=Tc1*Rc;

Tc2=[w2(1) -w2(2);
     w2(2) w2(1)];

Rc2_=Tc2*Rc;
Rcg1=b+q;

%Velocity
Rcg1d=q1d*e2 + omega1*[-Rc1_(2);Rc1_(1)];
Rcg2d=q2d*e2 + omega2*[-Rc2_(2);Rc2_(1)];

%%Acceleration
Rcg1dd=q1dd*e2 + alfa1*[-Rc1_(2);Rc1_(1)]-Rc1_*omega1^2;
Rcg2dd=q2dd*e2 + alfa2*[-Rc2_(2);Rc2_(1)]-Rc2_*omega2^2;
%%--------------------------------------------------------------------------
%%
%%Evaluation of the forces acting on each linkage

 Fext=[0 0]';
 Mext=0;
 Rcp=[0 0]';
 AID=[ 1       0          1       0   ;
       0       1          0       1   ;
      -yy      xx        -yy      xx  ;
      -l2*w1(2) l2*w1(1)   0        0   ;
       0       0         -l2*w2(2) l2*w2(1)];

  BID=[-M*rdd(1)+Fext(1);
       -M*rdd(2)+Fext(2)-M*g;
       -M*g*Rcp(1) + Mext + M*rdd(1)*Rcp(2)-M*rdd(2)*Rcp(1);
        m1*g*Rc1_(1)+m1*(Rcg1dd(1)*(-Rc1_(2))+Rcg1dd(2)*Rc1_(1))+J1*alfa1;
        m2*g*Rc2_(1)+m2*(Rcg2dd(1)*(-Rc2_(2))+Rcg2dd(2)*Rc2_(1))+J2*alfa2];

  FA=AID\BID;
     FA1=[FA(1) FA(2)]';
     FA2=[FA(3) FA(4)]';

 FB1(:,i)=-m1*g-FA1+m1*Rcg1dd;
 FB2(:,i)=-m2*g-FA2+m2*Rcg2dd;

 Fd1(1,i)=FB1(2,i)+ (ms+mcy)*q1dd;
 Fd2(1,i)=FB2(2,i)+ (ms+mcy)*q2dd;
end
%%--------------------------------E--N--D----------------------------------
```

1. Part II –Simulink Blocks Detail

2.1 Main Simulink model of the manipulator for kinematic analysis

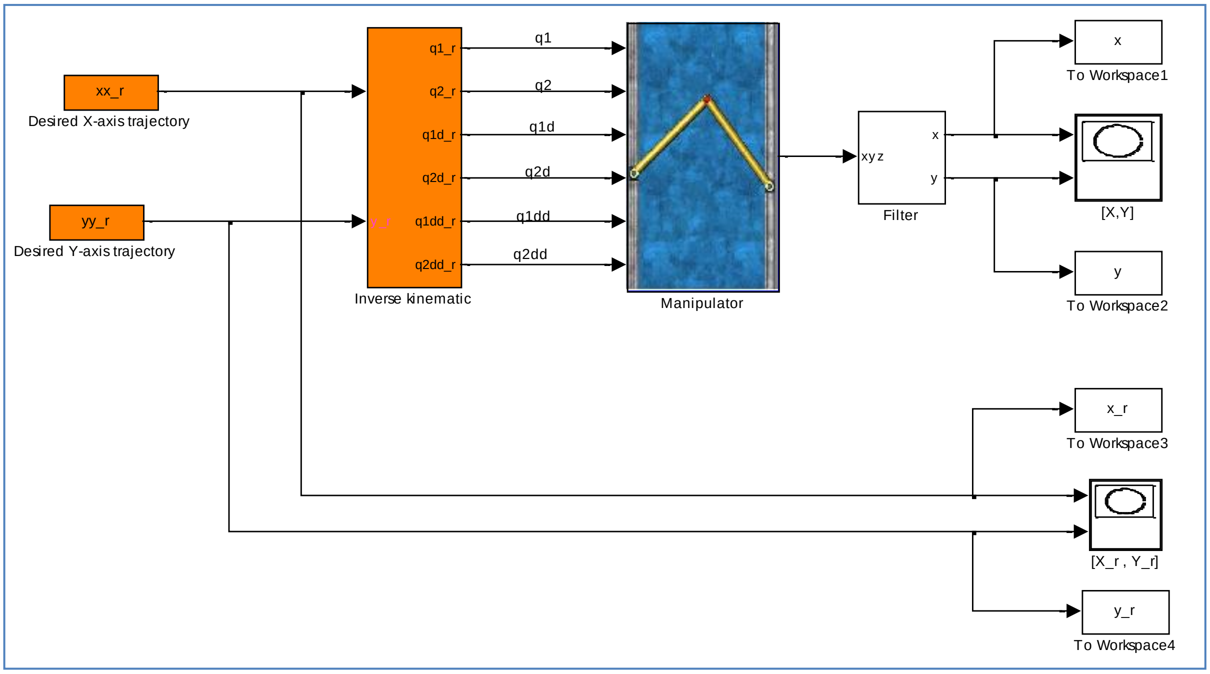

2.1.1 Inverse Kinematic Block

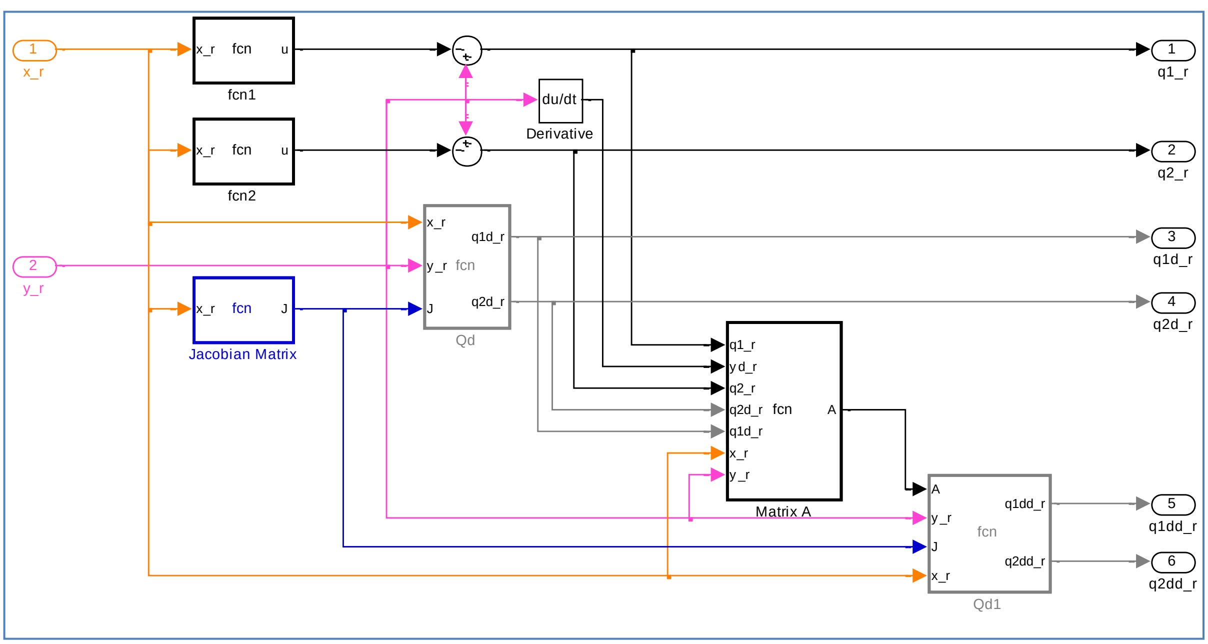

2.1.2 Manipulator Block

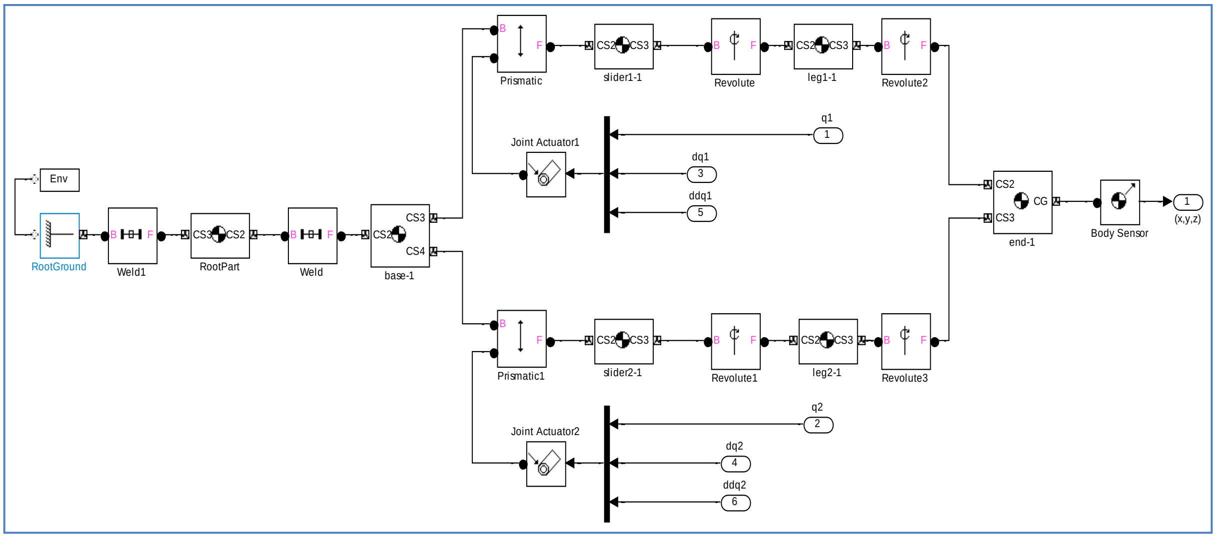

2.2 Main Simulink of the Manipulator for Dynamic Analysis

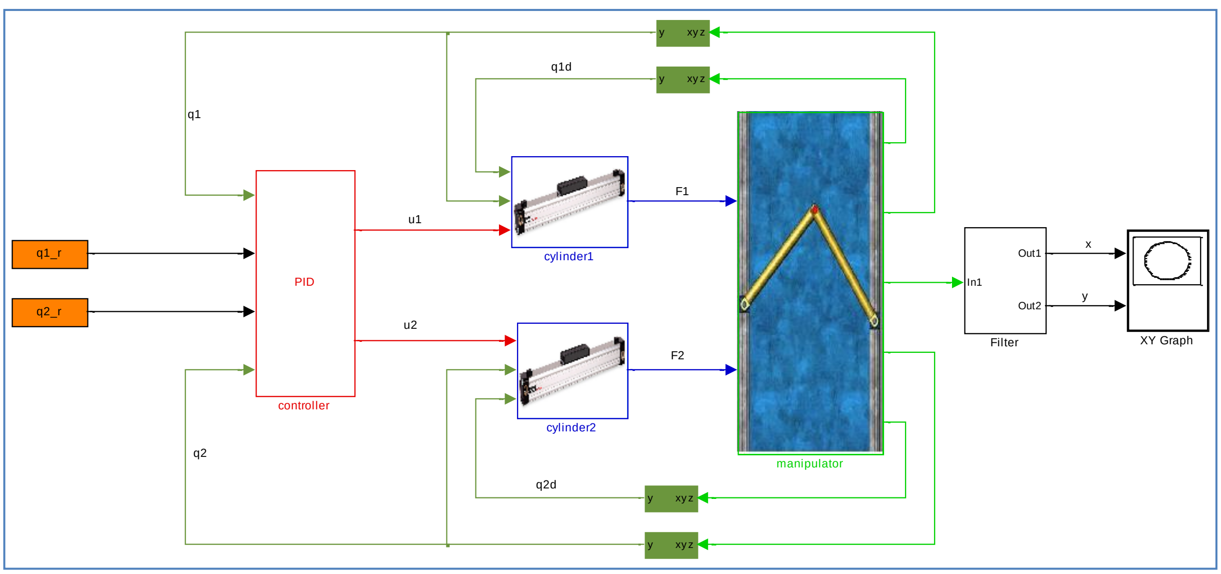

2.2.1 Controller Block

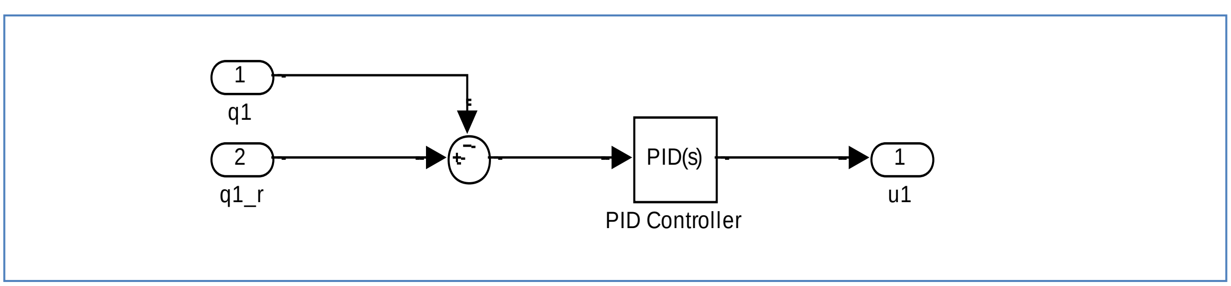

2.2.1.1 PID Block

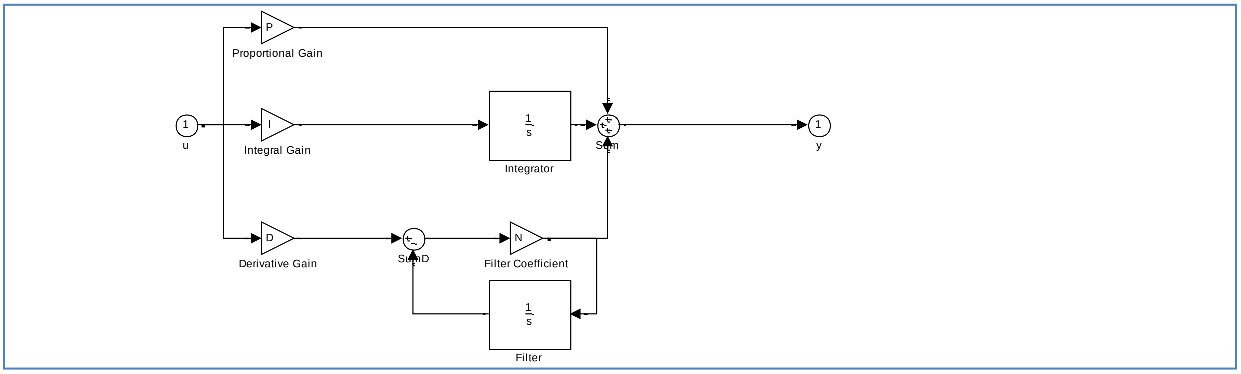

2.2.2 Cylinder Block

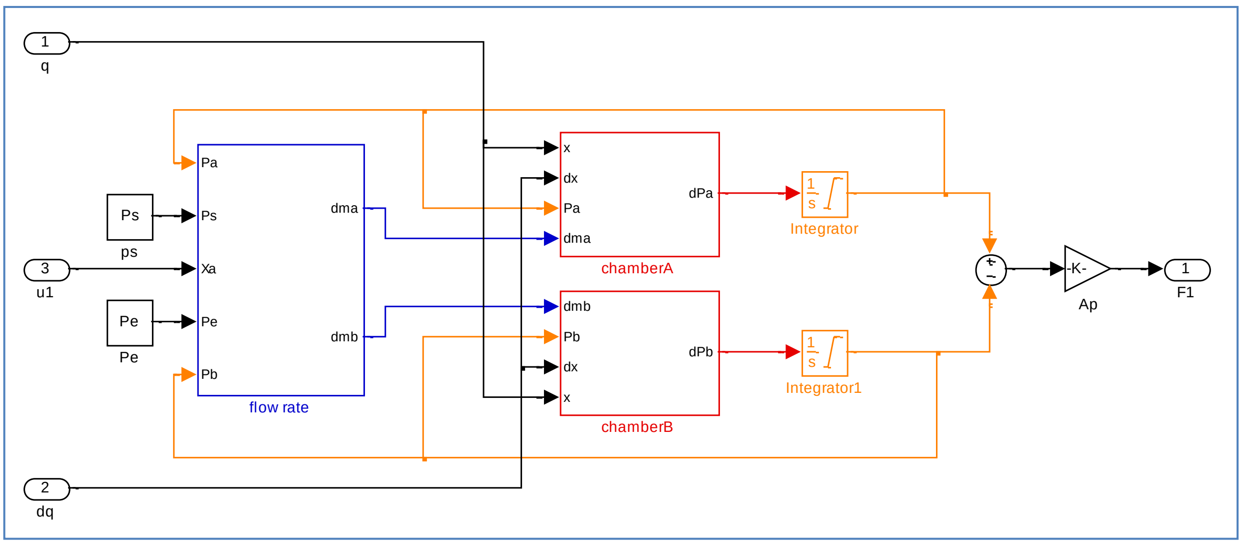

2.2.1.1 Flow rate Block

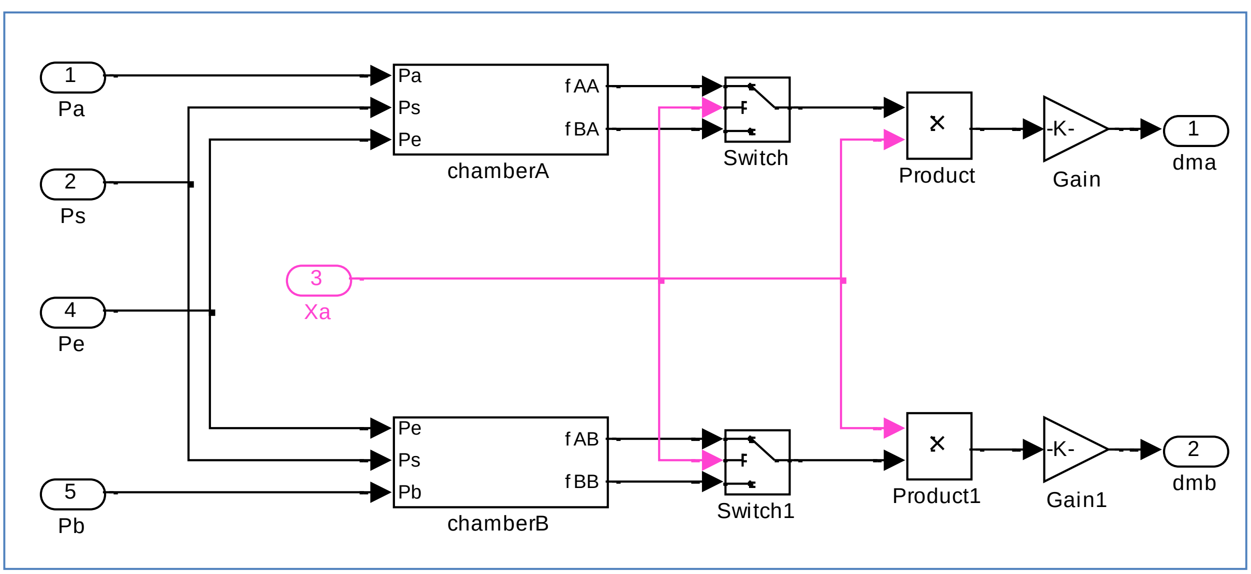

2.2.1.2 Block Diagram for Chambers Under the Flow rate Block

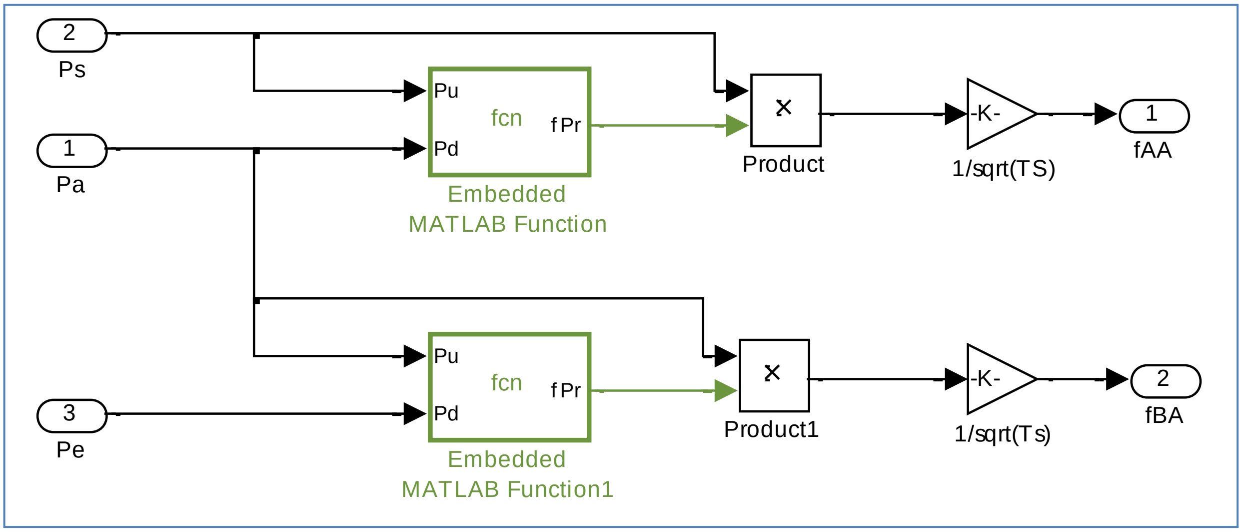

2.2.2 Chamber Block Under Cylinder Block Diagram

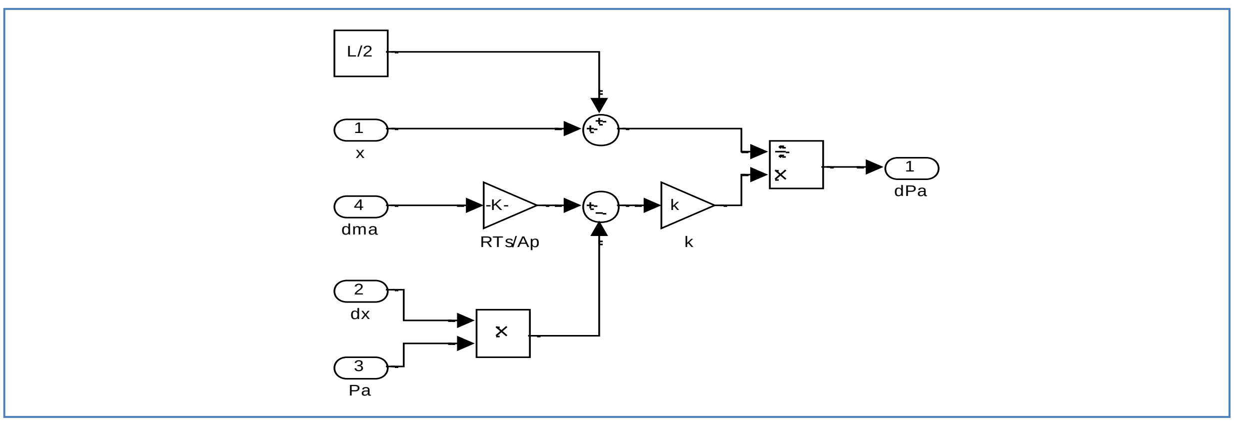

References

[1] Lui X-J., Wang Q-M. and Wang J. ''Kinematic, Dynamic and Dimensional Synthesis of a Novel 2 DoF Translational Manipulator''. *Journal of Intelligent and Robotic Systems 41, 205-224, 2004*

[2] Lui X., Wang J. and Pritschow G. ''On the optimal kinematic design of a PRRRP 2-DoF parallel mechanism''. *Mechanisms and Machine Theory 41, 1111-1130*, 2006

[3] Wu J., Li T., Lui X. And Wang L. ''Optimal kinematic design of a 2-DOF parallel manipulator''. *Tsinghua Science and Technology 12(3), 269-275*, 2007

[4] Sergiu-Dan S., Maties V. and Balan R. '' A multi criteria approach for the optimal design of 2 dof parallel robots used in construction applications''.*24th International Symposium on Automation & Robotics in Construction*, 2007

[5] Wang L-P., Wang J-S. and Chen J. ''The dynamic analysis of a 2-PRR planar parallel mechanism''. *Journal of Mechanical Engineering Science Vol. 219 Part C*, 2005

[6] Sergiu-Dan S., Maties V. and Balan R. '' Multi-objective Design Optimization of Mini Parallel Robots Using Genetic Algorithms''. *IEEE 1-4244-0755-9/0*, 2007

[7] Wu J., Wang J., Li T. and Wang L.'' Analysis and Application of a 2-DOF Planar Parallel Mechanism''. *ASME Journal of Mechanical design Vol. 129,* April 2007

[8] Wang L-P., Wang J-S., Li Y-W. amd Lu Y. '' Kinematic and dynamic equations of a planar parallel manipulator''. *Journal of Mechanical Engineering Science Vol.217 Part C, 2003*

[9] Yui Y.K., Cheng H., Xiong Z.H., Liu G.F. and Li Z.X. ''On the Dynamics **of** Parallel Manipulators''. *Proceedings of the 2001 IEEE international Conference on Robotics & Automation*, May 21-26, 2001

[10] Sorli M., Gastaldi L., Codina E. and de la Heras S. ''Dynamic analysis of pneumatic actuators''. *Simulation Practice and Theory 7, 589-602*, 1999

[11] Richer E. and Hurmuzlu Y. ''a high performance pneumatic force actiator system: part I-

Nonlinear mathematical model''. *Journal of Dynamic Systems, Measurement, and Control Vol. 122,* September 2000

[12] Kothapalli G. and Hassan Y. ''Design of a Neural Network Based Intelligent PI Controller for a Pneumatic System''. *IAENG International Journal of Computer Science, 35:2,* 20 May 2008

[13] Blagojevic V. and Stojiljkovic M. ''Mathematical and Simulink model of the pneumatic system with bridging of the dual action cylinder chambers''. *FACTA UNIVERSITATIS: Mechanical Engineering Vol.5 No1, pp 23-31,* 2007

[14] Fok S.C. and Ong E.K. '' Position control and repeatability of a pneumatic rodless cylinder continuous positioning'', *Robotics and Computer Integrated Manufacturing Vol. 15, 365-371,* 1999

[15] Sobczyk S., Mario R. and Eduardo A. ''Variable structure cascade control of a pneumatic positioning system''. *ABCM Symposium Series in Mechatronics Vol.2, 27-34,* 2006

[16] Chen C.K. and Hwang J. ''Iterative learning control for position tracking of a pneumatic actuated X–Y table''. *Control Engineering Practice 13, 1455-1461,* 2005

[17] Yu S.J., Qi X.D., Han R.C. and Pan F. ''Practical Design of an Iterative Learning-Sliding Mode Controller for Electro-Pneumatic''. *International Journal of Information Technology Vol. 11no. 5*

[18] Smaoui M., Brun X. and Thomasset D. ''Systematic Control of an Electro-pneumatic System: Integrator Backstepping and Sliding Mode Control''. IEEE Transactions on control systems technology, vol. 14, no. 5, september 2006

[19] Situm Z., Petric J. and Crnekovic M. ''Sliding Mode Control Applied to Pneumatic Servo Drive'' *Department of Automatic Control, Faculty of Mechanical Engineering and Naval Architecture, University of Zagreb*

[20] Wang J., Kotta U. and Ke J. ''Tracking control of nonlinear pneumatic actuator systems using static state feedback linearization of the input–output map''. *Proceeding of Estonian Academic for Science Physics and Mathematics, Vol. 56, No. 1, 47–66,* 2007

[21] Errahimi F., Cherrid H., Sirdi N.K.M. and Abarkane H. '' Robust adaptive control and observer for a robot with pneumatic actuators''. *Cambridge University Press: Robotica Vol. 20, 167-173,* 2002

[22] Spong M.W., Hutchison S. and Vidyasagar M. ''Robot Modeling and Control''. *JOHN WILEY & SONS, INC.*

[23] Giberti H., Chatterton S. and Cinquemani S. ''Kinematic Optimization of a Parallel Manipulator 5R 2-dof Driven by Pneumatic Cylinders''. *Dipartimento di Meccanica, Politecnico di Milano, Italy*

[24] Briot S. and Bonev I.A. ''Are parallel robots more accurate than serial robots?'' *CSME Transactions Vol 31, No 4, 445-456,* 2007

[25] Shang W.W., Cong S. and Jiang S.L. ''Dynamic model based nonlinear tracking control of a planar parallel manipulator''. *Springer Science+Business Media,* 2009

[26] Merlet J-P. ''Solving the forward kinematics of a Gough-type parallel manipulator with interval analysis''. *The International Journal of Robotics Research Vol. 23, No. 3, 221-235,* March 2004

[27] Bardat C., Nabat V., Company O., Krut S. and Pierrot F. ''Par2: a Spatial Mechanism for Fast Planar, 2-dof, Pick-and-Place Applications''. Proceedings of the Second International Workshop on *Fundamental Issues and Future Research Directions for Parallel Mechanisms and Manipulators.* September 21–22, 2008

[28] Huynh P., Arai T., Koyachi N. and Sendai T. ''Optimal Velocity based control o parallel manipulator with fixed linear actuators''. *IEEE:-Proc. IROS 97,* 1997

[29] Wang Z., Wang Z., Liu W. and Lei Y. ''A study on workspace, boundary workspace analysis and workpiece positioning for parallel machine tools''. *Elsevier Science: Mechanisms and Machine Theory Vol. 36, 605-622,* 2001

[30] Ali H.I., Noor S.B.M., Bashi S.M. and Marhaban M.H. ''A review of pneumatic actuators (modeling and control)''. *Australian Journal of basic and applied Sciences Vol. 3(2), 440-454,* 2009

[31] Najafi F., Fathi M. and Saadat M. ''Dynamic modeling of servo pneumatic actuators with cushioning''. *International Journal of Advanced Manufacturing Technologies Vol. 42, 757-765,* 2009

[32] Khayati K., Bigras P. and Dessaint L.A. ''Nonlinear control of pneumatic systems''. *École de Technologie Supérieure,214-220,*

[33] Richer E. and Hurmuzlu Y. ''a high performance pneumatic force actiator system: part II-Nonlinear control design''. *Journal of Dynamic Systems, Measurement, and Control Vol. 122,* September 2000

[34 Lee H.K., Choi G.S. and Choi G.H. ''A study on tracking position control of pneumatic actuators''. *Elsevier Science: Mechatronics Vol. 12, 813–831,* 2002

[35] Llagostera H.M. ''Control of a pneumatic servosystem using fuzzy logic'' *Proc. of 1st FPNI-PhD Sym., pp. 189-20, 2000. Hamburg*

[36] Papoutsidakis M.G., Chamilothoris G. and Pipe a. ''Auto-Selective Three Term Control of Position and Compliance of a Pneumatic Actuator''. *World Academy of Science, Engineering and Technology 26,* 2007

[37] Ilchemann A., Sawodny O. and Trenn S. ''Pneumatic cylinders: modeling and feedback force-control''. *Technische Universit¨at Ilmenau,*2 May 2005

[38] Nouri B.M.Y., Al-Bender F., Swevers J., Vanherck P. and Van Brussel H. ''Modeling a pneumatic servo positioning system with friction''. *Preceedings of the American control Conference,* 2000, Chicago, Illinois

[39] Zhu X., Cao J., Tao G. and Yao B. ''Synchronization Strategy Research of Pneumatic Servo System Based on Separate Control of Meter-in and Meter-out''. *IEEE/ASME International Conference on Advanced Intelligent Mechatronics,* July 14-17, 2009

[40] Gelezevicius V. and Grigaitis A. ''Research of Adaptive Force Control Loop of Electropneumatic Acting System'' *Electronics and Electrical Engineering No 7(79)* , 2007

[41] Sandler Ben-Z. ''Robotics: Designing the mechanisms for automated machinery'', *Second edition*, *Academic Press*, 1991

[42] Xie M. ''Fundamentals of Robotics: Linking Perception to Action'', *Machine Perception Artificial Intelligent Vol 54, World Scientific publishing Co. Pte. Ltd., 2003*

[43] Gibilisco Stan, ''Concise Encyclopedia of robotics'', *MacGraw-Hill,* 2003

[44] FESTO, Rodless drive units DGP/DGPL

[45] FESTO, End position controllers SPC11, Peripherals overview

[46] Stan Sergiu-Dan (Dr.). ''What is a Parallel Manipulator? ''. Senior Lecture Notes, Technical University of Cluj-Napoca Department of Mechanisms, Precision Mechanics and

[47] Corke Peter I. ''Robotics TOOLBOX for Matlab, release 6**'',** *CSIRO Manufacturing Science and Technology,* 2001.

[48] Wood G.D. and Kennedy D.C., ''Simulation Mechanical Systems in Simulink with SimMechanics'', The MathWorks

[49] FESTO DGP/DGPL, *Rodless double-acting pneumatic linear actuator*, Rodless Actuators Basic Version, Metric Series

[50] FESO, *Proportional directional control valves MPYE*, 5/3-way valve function